ANALYSIS OF VIRTUAL PASSIVE CONTROLLERS FOR FLEXIBLE SPACE STRUCTURES

NAG-1-1284

Final Report

Period of Research: June, 1991 - December, 1992

Principal Investigator: Trevor W. Williams, Associate Professor
Department of Aerospace Engineering

Technical Monitor: Jer-Nan Juang, Principal Scientist
Spacecraft Dynamics Branch

Abstract

The dynamics of flexible spacecraft are not usually well known before launch. This makes it important to develop controllers for such systems that can never be destabilized by perturbations in the structural model. Virtual passive controllers, or active vibration absorbers, possess this guaranteed stability property; they mimic a fictitious flexible structure attached to the true physical one.

This report analyzes the properties of such controllers, and shows that their disturbance absorption behavior can be naturally described in terms of a set of virtual zeros that they introduce into the closed-loop dynamics of the system. Based on this analysis, techniques are then derived for selecting the active vibration absorber internal parameters, i.e. the gain matrices of such controllers, so as to achieve specified control objectives.

Finally, the effects on closed-loop stability of small delays in the feedback loop are investigated. Such delays would typically be introduced by a digital implementation of an active vibration absorber. It is shown that these delays only affect the real parts of the eigenvalues of a lightly-damped structure. Furthermore, it is only the high-frequency modes that are destabilized by delays; low-frequency modes are actually made more heavily damped. Eigenvalue perturbation methods are used to obtain accurate predictions of the critical delay at which a given system will become unstable; these methods also determine which mode is critical.

TABLE OF CONTENTS

1. Introduction

An important practical difficulty in the control of flexible space structures (FSS) is that their dynamics are usually only poorly known. This is a consequence of the great difficulties involved in determining on-orbit behavior from pre-flight ground vibration tests. The sensitivity of an FSS control system to variations in the dynamics of the structure it is applied to is therefore a key practical consideration. A case that is particularly to be avoided is that of an unduly sensitive controller which gives good closed-loop performance for the nominal structure but destabilizes the true, off-nominal, vehicle.

Such considerations motivate the important class of *dissipative controllers* [1]. These control systems, based on the use of *compatible* (physically collocated and coaxial) actuators and rate sensors, guarantee closed-loop stability regardless of uncertainties present in the structural model. A related type of controller that has recently been proposed [2][3][16][17] is that of *virtual passive controllers*, in which the control system mimics a fictitious (or virtual) flexible structure attached to the physical structure to be controlled. The controller design problem then reduces to that of choosing the natural frequencies, damping ratios and mode shapes of this virtual structure in such a way as to satisfy the specifications placed on the closed-loop system. Such compensators are ideally suited to a high-authority/low-authority control scheme; they provide the stabilizing low-authority inner loop, so allowing a higher-performance feedback technique with no guaranteed stability, for instance a linear quadratic regulator (LQR), to be applied safely.

The first subject of this report is to develop methods for designing virtual passive controllers when the primary control objective is to achieve vibration absorption at various specified disturbance frequencies; the controller in this case is referred to as an *active vibration absorber* (*AVA*). This control objective amounts to requiring that *transmission zeros* [5] at these frequencies be introduced into the transfer functions between disturbance inputs and measured

outputs. A necessary preliminary step is therefore an analysis of the properties of the zeros of AVA-controlled flexible structures. The results obtained will be shown to be natural extensions of the open-loop FSS zeros relations of [4]; they also help to quantify the additional flexibility offered by AVA control over that provided by state feedback. Furthermore, this zeros analysis illuminates the significant differences between the case where the AVA sensor/actuator pairs are coincident with the disturbance sources or primary output sensors, and that where they are at distinct locations.

It should be noted that virtual passive controllers may be based on the use of compatible acceleration, rather than rate, measurements; this is the approach that will be taken here. The ease with which accelerometers can be distributed throughout a structure makes implementation of such a scheme extremely practical. Methods will then be derived for designing an accelerometer-based AVA which places the new *virtual zeros* at desired locations. The remaining design freedom is next quantified and exploited to satisfy some specified secondary control objectives, for instance minimization of the sensitivity of the closed-loop poles.

The effects on closed-loop stability of small delays in the feedback loop are also investigated in this report. Such delays would typically be introduced by any digital implementation of an active vibration absorber, so analysis of their effects is of great practical importance. First-order generalized eigenvalue perturbation methods are used to study these questions, and certain fundamental results obtained. As a first point, it is shown that delays acting on a lightly-damped flexible structure will basically only affect the real parts of the closed-loop eigenvalues. Furthermore, not all modes are destabilized by delays. Only the high-frequency modes are destabilized; the low-frequency modes are actually made more heavily damped. Accurate predictions are obtained of the critical delay at which a given system will become unstable; these methods also show which mode is the critical one. It should be noted that this will not necessarily simply be the highest-frequency mode of the structure. In fact, numerical simulations

suggest that this is very rarely the case. Finally, all the results obtained in this report are illustrated by application to simple examples. Further information on the work reported here is also given in [22].

2. AVA Equations

Consider an n-mode model for the structural dynamics of a non-gyroscopic, non-circulatory FSS acted on by low-authority control inputs **u**, disturbances **w** and high-authority control/reference signals **r**. This model can be written as

$$M\ddot{\mathbf{q}} + C\dot{\mathbf{q}} + K\mathbf{q} = B\mathbf{u} + B_D\mathbf{w} + B_H\mathbf{r},$$
$$\mathbf{y} = H_a\ddot{\mathbf{q}} + H_v\dot{\mathbf{q}} + H_d\mathbf{q}, \tag{2.1}$$

where the mass, stiffness and damping matrices satisfy $M = M^T > 0$, $K = K^T \geq 0$ and $C = C^T \geq 0$, respectively. The generalized coordinate vector **q** is (n x 1), **u** is (m x 1), and the measured output vector **y** is (p x 1).

A *virtual passive controller*, or *active vibration absorber (AVA)*, for this system is a low-authority controller which takes the form of a fictitious flexible structure attached to the physical structure. This can be written in modal form as

$$\ddot{\boldsymbol{\eta}}_v + diag(2\zeta_{vi}\omega_{vi})\dot{\boldsymbol{\eta}}_v + diag(\omega_{vi}^2)\boldsymbol{\eta}_v = \Phi_v^T\mathbf{u}_v, \tag{2.2}$$

where $\boldsymbol{\eta}_v$ is (n_V x 1) with $n_V \neq n$ in general. The input to this virtual system consists of m accelerometer measurements from the physical structure, collocated with the low-authority actuator stations,

$$\mathbf{u}_v = B^T\ddot{\mathbf{q}}. \tag{2.3}$$

Accelerometers are small, accurate and inexpensive, making them extremely suitable for practical use. This is the reason for the selection of acceleration feedback here. It should be noted, though, that displacement feedback would have to be added if rigid-body modes were to be controlled also. The analysis required in that case is entirely analogous to that which follows, and so will not be given explicitly.

The outputs from the virtual structure are m acceleration measurements, by analogy with the physical measurements, and collocated with its input stations,

$$\mathbf{y}_v = \Phi_v \ddot{\boldsymbol{\eta}}_v. \tag{2.4}$$

The manner in which the resulting low-authority control signals are applied to the physical system, i.e. the interconnection between the virtual and physical structures, is given as

$$\mathbf{u} = \mathbf{y}_v - G\mathbf{u}_v, \tag{2.5}$$

where the positive semi-definite symmetric gain matrix $G = \Phi_v \Phi_v^T$ is chosen so as to ensure stability of the closed-loop system regardless of perturbations in the FSS open-loop dynamics.

Combining (2.1) and (2.2) gives the composite equations of motion

$$\begin{pmatrix} M & 0 \\ 0 & I \end{pmatrix} \ddot{\overline{\mathbf{q}}} + \begin{pmatrix} C & 0 \\ 0 & diag(2\zeta_{vi}\omega_{vi}) \end{pmatrix} \dot{\overline{\mathbf{q}}} + \begin{pmatrix} K & 0 \\ 0 & diag(\omega_{vi}^2) \end{pmatrix} \overline{\mathbf{q}}$$

$$= \begin{pmatrix} B\mathbf{u} + B_D\mathbf{w} + B_H\mathbf{r} \\ \Phi_v^T \mathbf{u}_v \end{pmatrix}, \tag{2.6}$$

where $\overline{\mathbf{q}} = \begin{pmatrix} \mathbf{q}^T & \boldsymbol{\eta}_v^T \end{pmatrix}^T$. Using (2.3) - (2.5), the right-hand side can be rewritten as

$$\begin{pmatrix} B[\mathbf{y}_v - G\mathbf{u}_v] + B_D\mathbf{w} + B_H\mathbf{r} \\ \Phi_v^T\mathbf{u}_v \end{pmatrix}$$

$$= \begin{pmatrix} B\Phi_v\ddot{\eta}_v - BGB^T\ddot{\mathbf{q}} + B_D\mathbf{w} + B_H\mathbf{r} \\ \Phi_v^T B^T\ddot{\mathbf{q}} \end{pmatrix}. \tag{2.7}$$

Taking all terms involving **x** to the left-hand side then yields the closed-loop equations of motion

$$\overline{M}\ddot{\overline{\mathbf{q}}} + \overline{C}\dot{\overline{\mathbf{q}}} + \overline{K}\overline{\mathbf{q}} = \overline{B}_D\mathbf{w} + \overline{B}_H\mathbf{r},$$

$$\mathbf{y} = \overline{H}_a\ddot{\overline{\mathbf{q}}} + \overline{H}_r\dot{\overline{\mathbf{q}}} + \overline{H}_d\overline{\mathbf{q}}, \tag{2.8}$$

where

$$\overline{M} = \begin{pmatrix} [M + B\Phi_v\Phi_v^T B^T] & -B\Phi_v \\ -\Phi_v^T B^T & I \end{pmatrix},$$

$$\overline{C} = \begin{pmatrix} C & 0 \\ 0 & diag(2\zeta_{vi}\omega_{vi}) \end{pmatrix} \tag{2.9}$$

and

$$\overline{K} = \begin{pmatrix} K & 0 \\ 0 & diag(\omega_{vi}^2) \end{pmatrix}.$$

Similarly, $\overline{B}_D = \begin{pmatrix} B_D^T & 0 \end{pmatrix}^T$, $\overline{H}_a = \begin{pmatrix} H_a & 0 \end{pmatrix}$, etc. To simplify the notation in what follows, we define the (n x n_V) matrix $X \equiv B\Phi_v$. The composite mass matrix then becomes

$$\overline{M} = \begin{pmatrix} [M + XX^T] & -X \\ -X^T & I \end{pmatrix}. \tag{2.10}$$

Now, the composite stiffness and damping matrices are positive semi-definite, by inspection. Defining the gain matrix G as in (2.5) ensures that $\overline{M}$ is also actually positive definite, so guaranteeing that the composite equations of motion (2.8) represent the dynamics of a flexible structure. Positive definiteness can be proved as follows: for any $\overline{\mathbf{q}} = \begin{pmatrix} \mathbf{q}^T & \eta_v^T \end{pmatrix}^T$ we have

$$\begin{aligned}\overline{\mathbf{q}}^T\overline{M}\overline{\mathbf{q}} &= \mathbf{q}^T(M+XX^T)\mathbf{q} - 2\mathbf{q}^T X\boldsymbol{\eta}_v + \boldsymbol{\eta}_v^T\boldsymbol{\eta}_v \\ &= \mathbf{q}^T M\mathbf{q} + (X^T\mathbf{q}-\boldsymbol{\eta}_v)^T(X^T\mathbf{q}-\boldsymbol{\eta}_v) \\ &\equiv \mathbf{q}^T M\mathbf{q} + \mathbf{z}^T\mathbf{z} > 0,\end{aligned} \tag{2.11}$$

as $M > 0$. Thus, the closed-loop poles produced by the AVA will be stable, regardless of any perturbations in the open-loop dynamics (2.1). It is interesting to note that the vector $\mathbf{z}$ is closely related to the control signal applied to the physical structure by the AVA: this is just, by (2.3) - (2.5),

$$\mathbf{u} = -\Phi_v[X^T\ddot{\mathbf{q}} - \ddot{\boldsymbol{\eta}}_v] = -\Phi_v\ddot{\mathbf{z}}. \tag{2.12}$$

The AVA design problem to be studied in this paper can be stated as follows: select the parameters $\{\omega_{vi}\}$, $\{\zeta_{vi}\}$, Φ_v and B (i.e. the AVA sensor/actuator locations) so as to minimize the frequency response magnitude of the closed-loop measured outputs $\{y_i\}$ at some specified frequencies. These frequencies will typically be those at which the harmonic disturbance inputs $\{w_j\}$ are expected to occur. This vibration isolation problem will be considered to be the primary control objective; any additional design freedom available will then be used to satisfy other secondary objectives, for instance minimization of the sensitivity of the closed-loop poles to perturbations in the plant.

The vibration isolation problem is equivalent to requiring that *transmission zeros* [5] be introduced, at the specified disturbance frequencies, into the transfer functions of the composite system between specified disturbances and specified outputs. It will be shown below that the solution of this question depends centrally on whether the AVA sensor/actuator pairs can be coincident with either the disturbance sources or the measured output ($\mathbf{y}$) sensors. In order to fully investigate the solution methods and properties in the two cases, they will be considered separately in the two sections that follow.

3. Coincident Case

The properties of the zeros of a flexible structure controlled by an AVA have not been studied to date. This analysis will now be given as a necessary basis for the results to follow. It will also serve to illuminate the differences between the case where the AVA is coincident with the disturbances or measured outputs and the general non-coincident arrangement.

Taking the Laplace transform of (2.8) gives the *polynomial matrix representation* [8]

$$\begin{aligned} \overline{P}(s)\overline{\mathbf{q}}(s) &= \overline{B}_D\mathbf{w}(s) + \overline{B}_H\mathbf{r}(s), \\ \mathbf{y}(s) &= \overline{H}(s)\overline{\mathbf{q}}(s), \end{aligned} \tag{3.1}$$

for the composite system, where $\overline{P}(s) = s^2\overline{M} + s\overline{C} + \overline{K}$ and $\overline{H}(s) = s^2\overline{H}_a + s\overline{H}_r + \overline{H}_d$. The transmission zeros of this system between disturbance input j and measured output i are those values of s for which the rank of the *system matrix* [5]

$$S(s) = \begin{pmatrix} \overline{P}(s) & \overline{\mathbf{b}}_j \\ -\overline{\mathbf{h}}_i(s) & 0 \end{pmatrix} \tag{3.2}$$

is reduced. This polynomial matrix definition is more convenient to deal with than the rational one involving the *transfer function* $T_{ij}(s) = \overline{\mathbf{h}}_i(s)\overline{P}(s)^{-1}\overline{\mathbf{b}}_j$; so long as the input-output loop examined is completely controllable and observable, the results obtained are the same in both cases.

These zeros can be studied by means of a generalization of the method employed in [4][6][9] to investigate the zeros of open-loop flexible structures. This makes use of the *QR decompositions* [7] of $\mathbf{b}_j$ and $\mathbf{h}_i^T$, i.e. $\mathbf{b}_j = Q_b\mathbf{r}_b = (\mathbf{q}_{b1} \quad Q_{b2})(\rho_b \quad 0 \quad \cdots \quad 0)^T$ and $\mathbf{h}_i^T = Q_h\mathbf{r}_h = (\mathbf{q}_{h1} \quad Q_{h2})(\rho_h \quad 0 \quad \cdots \quad 0)^T$, with Q_b and Q_h both orthogonal matrices and ρ_b, ρ_h non-zero scalars. Applying these transformations to $S(s)$ allows it to be reduced to a canonical form from which the transmission zeros can be obtained by inspection. In particular,

$$\left(\begin{array}{cc|c} Q_b^T & 0 & \mathbf{0} \\ 0 & I & \mathbf{0} \\ \hline \mathbf{0} & \mathbf{0} & 1 \end{array}\right) S(s) \left(\begin{array}{cc|c} Q_h & 0 & \mathbf{0} \\ 0 & I & \mathbf{0} \\ \hline \mathbf{0} & \mathbf{0} & 1 \end{array}\right)$$

$$= \left(\begin{array}{c|c} \begin{pmatrix} Q_b^T & 0 \\ 0 & I \end{pmatrix} \overline{P}(s) \begin{pmatrix} Q_h & 0 \\ 0 & I \end{pmatrix} & \begin{pmatrix} Q_b^T & 0 \\ 0 & I \end{pmatrix} \begin{pmatrix} \mathbf{b}_j \\ \mathbf{0} \end{pmatrix} \\ \hline -(\mathbf{h}_i \quad \mathbf{0}) \begin{pmatrix} Q_h & 0 \\ 0 & I \end{pmatrix} & 0 \end{array}\right)$$

$$= \left(\begin{array}{c|c} \begin{pmatrix} Q_b^T & 0 \\ 0 & I \end{pmatrix} \overline{P}(s) \begin{pmatrix} Q_h & 0 \\ 0 & I \end{pmatrix} & \begin{pmatrix} \rho_j \\ \mathbf{0} \end{pmatrix} \\ \hline -(\rho_i \quad \mathbf{0}) & 0 \end{array}\right). \tag{3.3}$$

As ρ_b and ρ_h are non-zero, the first row and column of this matrix may be omitted when searching for values of s which make it singular. Thus, the zeros are just those values for which

$$\hat{S}(s) = \begin{pmatrix} Q_{b2}^T & 0 \\ 0 & I \end{pmatrix} \overline{P}(s) \begin{pmatrix} Q_{h2} & 0 \\ 0 & I \end{pmatrix} \tag{3.4}$$

has less than full rank.

So far, collocation of AVA and disturbance has not been assumed. The effect of making this restriction is to obtain a transformed system matrix which is block triangular, leading to a simple decomposition result for the resulting zeros. In detail, if $B = \mathbf{b}_j$ then $X = \mathbf{b}_j \Phi_v$, so $Q_{b2}^T X = 0$. Thus, by (2.10) we have

$$\begin{pmatrix} Q_{b2}^T & 0 \\ 0 & I \end{pmatrix} \overline{M} \begin{pmatrix} Q_{h2} & 0 \\ 0 & I \end{pmatrix} = \begin{pmatrix} Q_{b2}^T M Q_{h2} & 0 \\ -X Q_{h2} & I \end{pmatrix}; \tag{3.5}$$

also, $\begin{pmatrix} Q_{b2}^T & 0 \\ 0 & I \end{pmatrix} \overline{C} \begin{pmatrix} Q_{h2} & 0 \\ 0 & I \end{pmatrix}$ and $\begin{pmatrix} Q_{b2}^T & 0 \\ 0 & I \end{pmatrix} \overline{K} \begin{pmatrix} Q_{h2} & 0 \\ 0 & I \end{pmatrix}$ are block diagonal by inspection. $\hat{S}(s)$ is therefore indeed block lower triangular, of the form

$$\hat{S}(s) = \begin{pmatrix} Q_{b2}^T [s^2 M + sC + K] Q_{h2} & 0 \\ -s^2 X Q_{h2} & P_v(s) \end{pmatrix}, \tag{3.6}$$

where $P_v(s) = s^2 I + s \cdot diag\{2\zeta_{vi}\omega_{vi}\} + diag\{\omega_{vi}^2\}$. The top left block of this equation can be seen to be just the polynomial matrix which defines the *structural zeros* [4] of the open-loop physical flexible structure, while the lower right block is the denominator matrix of the AVA virtual structure.

The zeros of the composite system between disturbance j and output i are therefore made up of three distinct sets:

(a) the *sensor zeros*, consisting of a single zero at the origin for a rate measurement, and two for acceleration;

(b) the structural zeros of the SISO open-loop physical system for this disturbance/output pair;

(c) the poles of the virtual system (2.2). These will be referred to as the *virtual zeros* of the composite system.

The first two sets of zeros are independent of the choice of AVA parameters; they are just those zeros which the open-loop physical structure initially possessed. Adding closed-loop zeros at desired frequencies is therefore achieved by placing the poles of the virtual structure at these locations. This makes sense physically, as the virtual system will then resonate at these frequencies, so absorbing energy and minimizing vibration. It should be noted that this result is entirely independent of the parameters of the open-loop physical structure; it holds whenever the disturbance source and AVA sensor/actuator pair are coincident. It will be shown in the next section that the results that hold in the non-coincident case are not so simple; in particular, they do depend on the open-loop model.

It is well known [5] that the zeros of a given system cannot be altered in any way by state feedback. Thus, AVA control provides an additional degree of design freedom over that provided by state feedback. The virtual zeros are, in fact, closely related to the *disturbance zeros* defined in [10] for the case of dynamic output feedback. However, that paper did not examine flexible structure applications or properties.

It was assumed above that the AVA was coincident with the disturbance source of interest. An entirely similar result applies if the AVA is instead coincident with the output sensor. (The transformed system matrix $\hat{S}(s)$ is then block upper triangular rather than lower.) The poles of the virtual system again become the additional zeros of the composite system, and the only significant difference appears when the problem is generalized to the multi-disturbance/multi-output case. An AVA which is coincident with disturbance j can be used to introduce a zero at this disturbance frequency for arbitrary output locations. Thus, such an absorber provides "global" attenuation of this particular disturbance. By contrast, an AVA coincident with output sensor i can only absorb the disturbance at this physical location; the other outputs will still be affected by it. However, a compensation for this "local" attenuation is the fact that the AVA can now absorb multiple disturbances at this output station. In particular, an AVA of order n_V can isolate the output from n_V disturbances, generally acting at different frequencies and applied at different locations. This is a very powerful property.

We have therefore shown that, in the coincident case, the natural frequencies $\{\omega_{vi}\}$ of the virtual system should be chosen to be equal to the disturbance frequencies which are to be absorbed. Also, the absorber influence matrix B is constrained by the requirement that the AVA be coincident with either the disturbances or the outputs. Therefore, the only design variables remaining to be assigned are the damping ratios $\{\zeta_{vi}\}$ and modal matrix Φ_v. These may be selected as follows.

The level of virtual damping is chosen based on a trade-off which can be viewed in either the time or frequency domain. Decreasing the virtual damping gives a deeper trough in the frequency response of the composite system at the desired attenuation frequency; however, the trough is narrower, giving less robust vibration absorption in the event of perturbations in the disturbance frequency. Similarly, lower damping gives a smaller steady-state time response to a sinusoidal disturbance at the specified frequency, but at the expense of a longer decay time for the initial transients. An optimum choice for $\{\zeta_{vi}\}$ will therefore depend on the details of the particular application considered; as a general rule though, simulations to date indicate that values in the range 0.05 - 0.10 give good results.

The virtual influence matrix Φ_v can actually be chosen arbitrarily without altering the virtual zeros at all. It can therefore be regarded as making up a set of design variables which may be used to satisfy some secondary system requirement, over and above the primary one of vibration isolation. Of course, for the case of a single degree-of-freedom AVA, altering Φ_v amounts to a simple scaling of the virtual output $\mathbf{y}_v$; it can be shown to be dynamically equivalent to scaling the mass of the virtual system (2.2). In general, increasing Φ_v increases the gain matrix G (equation (2.5)), and so the control effort $\mathbf{u}$ (equation (2.12)); it is therefore essentially a control gain-type variable.

Two particular secondary design requirements will be investigated here: minimization of an 'LQR-like' steady-state error quantity, and minimization of the sensitivity of the poles of the closed-loop system. In the first case, the objective function is of the form

$$J = \|\mathbf{y}_{ss}\|_2^2 + \rho\|\mathbf{u}_{ss}\|_2^2, \tag{3.7}$$

where the system is excited by the harmonic disturbance signal. The control weighting ρ is used as in the standard LQR method to allow the relative importance of control effort and output

performance to be varied. In the second problem studied, the quantities to be minimized are the sensitivities of the poles of the composite system, i.e. the eigenvalues of

$$A = \begin{pmatrix} -\overline{M}^{-1}\overline{C} & -\overline{M}^{-1}\overline{K} \\ I & 0 \end{pmatrix}. \tag{3.8}$$

The sensitivity of the eigenvalue λ_i of A is measured by its *condition number* c_i, which is defined [11] as follows: if λ_i has corresponding right eigenvector $\mathbf{x}_i$ ($A\mathbf{x}_i = \lambda_i \mathbf{x}_i$) and left eigenvector $\mathbf{y}_i$ ($\mathbf{y}_i^H A = \lambda_i \mathbf{y}_i^H$), with $\|\mathbf{x}_i\|_2 = \|\mathbf{y}_i\|_2 = 1$, then its condition number is

$$c_i = 1/|\mathbf{y}_i^H \mathbf{x}_i|. \tag{3.9}$$

This quantity, which can be seen to be always greater than or equal to unity, measures the magnification between a perturbation in A and the resulting induced perturbation in λ_i. Choosing Φ_v so as to reduce the $\{c_i\}$ yields a closed-loop system which is robust as well as guaranteed stable; this is certainly desirable in practice, given the uncertainties inherent in FSS models. Examples of the use of both the methods just outlined for selecting Φ_v will be given later in the paper.

4. Non-Coincident Case

It may not always be possible in practice to place the AVA sensor/actuator pairs at either the disturbance sources or the primary output sensors. The closed-loop properties that then apply are, as has already been noted, considerably more complicated than those that held in the coincident case. In particular, the transmission zeros introduced by a non-coincident AVA are no longer simply equal to its own poles; a degree of dependency on the physical structure enters into the problem of choosing the AVA natural frequencies. This model-dependency is not unduly serious, however, as closed-loop stability is still guaranteed regardless of open-loop perturbations. (See [1] for a similar observation concerning positive real controllers.)

The analysis required in the non-coincident AVA case proceeds initially in the same manner as that given in the last section. Equations (3.2) - (3.4) apply entirely without change, and the extra complexity only arises when we apply the required transformations to the composite mass matrix $\overline{M}$. As $B \neq \mathbf{b}_j$ here we no longer have $Q_{b2}^T X = 0$, so $\overline{M}$ and $\hat{S}(s)$ are not block lower triangular. Instead, if we define the quantities

$$Y = Q_{b2}^T X$$

and (4.1)

$$Z = Q_{h2}^T X,$$

(2.10) implies that the transformed mass matrix becomes

$$\begin{pmatrix} Q_{b2}^T & 0 \\ 0 & I \end{pmatrix} \overline{M} \begin{pmatrix} Q_{h2} & 0 \\ 0 & I \end{pmatrix} = \begin{pmatrix} [Q_{b2}^T M Q_{h2} + YZ^T] & -Y \\ -Z^T & I \end{pmatrix}. \tag{4.2}$$

Consequently,

$$\hat{S}(s) = \begin{pmatrix} [Q_{b2}^T P(s) Q_{h2} + s^2 YZ^T] & -s^2 Y \\ -s^2 Z^T & P_v(s) \end{pmatrix}, \tag{4.3}$$

where $P(s) = s^2 M + sC + K$. Now, the transmission zeros of the composite system are those values of s which make $\hat{S}(s)$ singular. Thus, making use of the standard determinantal identity [12]

$$\det \begin{pmatrix} A & B \\ C & D \end{pmatrix} = \det\{A\} \cdot \det\{D - CA^{-1}B\} \tag{4.4}$$

for partitioned matrices, we have that any zero $\tilde{s}$ must either satisfy

$$\det\{Q_{b2}^T P(\tilde{s}) Q_{h2} + \tilde{s}^2 YZ^T\} = 0 \tag{4.5}$$

or

$$\det\{P_v(\tilde{s}) - \tilde{s}^4 Z^T [Q_{b2}^T P(\tilde{s}) Q_{h2} + \tilde{s}^2 Y Z^T]^{-1} Y\} = 0. \tag{4.6}$$

Note that, in the coincident case, either Y or Z is zero; (4.5) then reduces to the defining equation for the structural zeros of the physical structure, and (4.6) to $\det\{P_v(\tilde{s})\} = 0$, the defining equation for the virtual zeros. The results of the last section are therefore indeed a special case of those obtained here. The fact that the structural zeros depend on the applied feedback in the non-coincident case is analogous to the observation [13][14] that the zeros of a flexible structure can be shifted by dampers only if these are not coincident with the primary sensors and actuators.

The AVA design problem in the general case thus reduces to that of finding a $P_v(s) = s^2 I + s \cdot diag\{2\zeta_{vi}\omega_{vi}\} + diag\{\omega_{vi}^2\}$ which satisfies (4.6) for some desired closed-loop zero $\tilde{s}$. This equation becomes much simpler to solve when the AVA has a single degree-of-freedom ($n_v = 1$); Y and Z are then column vectors and $P_v(s)$ is a scalar, so (4.6) reduces to

$$P_v(\tilde{s}) = \tilde{s}^4 \mathbf{z}^T [Q_{b2}^T P(\tilde{s}) Q_{h2} + \tilde{s}^2 \mathbf{y}\mathbf{z}^T]^{-1} \mathbf{y}. \tag{4.7}$$

All quantities on the right-hand side are known, while the left-hand side is just $\tilde{s}^2 + 2\zeta_v \omega_v \tilde{s} + \omega_v^2$. Thus, we have a relation of the form

$$2\zeta_v \omega_v \tilde{s} + \omega_v^2 = \alpha + j\beta, \tag{4.8}$$

where $\tilde{s} = \sigma + j\tau$. The required virtual frequency and damping ratio are then given from the known quantities α, β, σ and τ as

$$\omega_v = \sqrt{\frac{\alpha\tau - \beta\sigma}{\tau}}$$

and (4.9)

$$\zeta_v = \frac{\beta}{2\omega_v \tau}.$$

These solutions always exist; however, they may be imaginary in certain cases, making the resulting $P_v(s)$ physically meaningless. Numerical results to date indicate that such infeasible solutions occur only when high gains (i.e. large Φ_v) are used and $\tilde{s}$ is positioned in the vicinity of a closed-loop structural zero. This choice of zero causes the matrix in (4.5) to be nearly singular, leading to numerical ill-conditioning problems when performing the inversion in (4.7). However, this case is very unlikely to arise in practice: if a structural zero is near the disturbance frequency, it will already provide sufficient attenuation. There will therefore be no need to place a new virtual zero there as well.

The multi-degree-of-freedom AVA problem must be solved using an entirely different approach, which will now be briefly described. For simplicity, we shall neglect the small amounts of damping present in both the original flexible structure and the desired virtual zeros $\{\tilde{s}_l : l = 1,\ldots,n_v\}$. The second matrix in (4.6), denoted by W_l say, is then clearly real. The solution $P_v(s)$ consequently proves to be undamped also, with natural frequencies which must satisfy

$$\det\{diag(\omega_{vi}^2) + [diag(\tilde{s}_l^2) + W_l]\} = 0, \tag{4.10}$$

$l = 1,\ldots,n_v$. These simultaneous determinantal equations may be readily solved using a symbolic manipulation package such as Mathematica [15], giving the required virtual natural frequencies. Of course, just as in the single degree-of-freedom case, these values may on occasion turn out to be imaginary, and so infeasible. The likelihood of this occurring in practice is a subject requiring further research.

5. Closed-Loop Equations with Delay

Introducing a delay into the feedback loop used to implement the AVA controller corrupts the symmetry of the composite mass, stiffness and/or damping matrices. This in turn prevents the unconditional, model-independent stability guarantees that held in the undelayed case.

In detail, if we assume a small delay τ in the feedback signal, we can use the first-order exponential approximation

$$e^{-s\tau} \approx 1 - s\tau \tag{5.1}$$

to compute the perturbed matrices of the closed-loop system. These are

$$M_\tau \approx \overline{M} + \tau\tilde{M}, \tag{5.2}$$

$$C_\tau \approx \overline{C} + \tau\tilde{C} \tag{5.3}$$

and

$$K_\tau \approx \overline{K}. \tag{5.4}$$

Note that the composite stiffness matrix is, to first order, unchanged by the introduction of the delay. The perturbation matrices are given as

$$\tilde{M} = \begin{pmatrix} 0 & -B\Phi_v diag(2\zeta_{vi}\omega_{vi}) \\ 0 & 0 \end{pmatrix} \tag{5.5}$$

and

$$\tilde{C} = \begin{pmatrix} 0 & -B\Phi_v diag(\omega_{vi}^2) \\ 0 & 0 \end{pmatrix}. \tag{5.6}$$

The important point to note is that neither of these matrices are symmetric. Thus, the closed-loop system obtained for a non-zero delay does <u>not</u> correspond to a composite fictitious flexible structure. It therefore does not possess guaranteed stability, as will now be demonstrated in more detail.

The delayed system has poles given by the roots of the characteristic equation

$$\det\{\lambda^2 M_\tau + \lambda C_\tau + K\} = 0. \tag{5.7}$$

This equation is not amenable to solution in its present form, as it is in terms of a polynomial, or *lambda*, matrix. To obtain useful numerical or analytical results, it must be transformed to a simpler first-order form. Two possible main approaches exist: to reduce it to a generalized eigenvalue problem of the form

$$A\mathbf{x} = \lambda B\mathbf{x}, \tag{5.8}$$

or to reduce it even further to a standard eigenvalue problem by inverting the matrix B. The generalized eigenvalue formulation is the option to be preferred here, as performing a matrix inversion corrupts and confuses the matrix perturbation expressions (3.2) - (3.6) that form the basis of the semi-closed-form results that will follow. Defining the state vector

$$\mathbf{x} = \begin{pmatrix} \dot{\overline{\mathbf{q}}} \\ \overline{\mathbf{q}} \end{pmatrix} \tag{5.9}$$

yields a generalized eigenvalue problem (5.8) for the delayed system (5.7), where

$$A = \begin{pmatrix} -C_\tau & -\overline{K} \\ I & 0 \end{pmatrix} \tag{5.10}$$

and

$$B = \begin{pmatrix} M_\tau & 0 \\ 0 & I \end{pmatrix}. \tag{5.11}$$

In terms of the perturbation expressions given previously, these matrices can be written as

$$A = A_0 + \delta A \tag{5.12}$$

and

$$B = B_0 + \delta B, \tag{5.13}$$

where

$$A_0 = \begin{pmatrix} -\overline{C} & -\overline{K} \\ I & 0 \end{pmatrix}, \delta A = \tau \cdot \begin{pmatrix} -\tilde{C} & 0 \\ 0 & 0 \end{pmatrix}, \tag{5.14}$$

$$B_0 = \begin{pmatrix} \overline{M} & 0 \\ 0 & I \end{pmatrix} \text{and } \delta B = \tau \cdot \begin{pmatrix} \tilde{M} & 0 \\ 0 & 0 \end{pmatrix}. \tag{5.15}$$

A recent perturbation result for the generalized eigenvalue problem (where such results are considerably more difficult to obtain than for the standard eigenvalue problem) can now be applied to these matrices. Suppose that $\mathbf{x}$ is the right eigenvector of the nominal generalized eigenproblem corresponding to eigenvalue λ, i.e. the solution of

$$A_0\mathbf{x} = \lambda B_0\mathbf{x}, \tag{5.16}$$

and $\mathbf{y}$ is the corresponding left eigenvector, i.e. the solution of

$$\mathbf{y}^H A_0 = \mathbf{y}^H \lambda B_0. \tag{5.17}$$

Then a first order approximation to the eigenvalue of the perturbed generalized eigenproblem (5.8), with A and B as given by (5.12) and (5.13), is [18]

$$\lambda + \delta\lambda \approx \mathbf{y}^H(A_0 + \delta A)\mathbf{x} \,/\, \mathbf{y}^H(B_0 + \delta B)\mathbf{x}. \tag{5.18}$$

Now, premultiplying (5.8) by $\mathbf{y}^H$ yields

$$\lambda = \mathbf{y}^H A_0\mathbf{x} \,/\, \mathbf{y}^H B_0\mathbf{x}. \tag{5.19}$$

Thus, we can rewrite and expand (5.18) as

$$\begin{aligned} (\lambda + \delta\lambda)\mathbf{y}^H(B_0 + \delta B)\mathbf{x} &\approx \lambda\mathbf{y}^H B_0\mathbf{x} + \lambda\mathbf{y}^H\delta B\mathbf{x} + \delta\lambda\mathbf{y}^H B_0\mathbf{x} \\ &\approx \mathbf{y}^H(A_0 + \delta A)\mathbf{x} \\ &= \lambda\mathbf{y}^H B_0\mathbf{x} + \mathbf{y}^H\delta A\mathbf{x}. \end{aligned} \tag{5.20}$$

The perturbation in the generalized eigenvalue λ can therefore be written, to first order, as

$$\delta\lambda \approx [\mathbf{y}^H\delta A\mathbf{x} - \lambda\mathbf{y}^H\delta B\mathbf{x}] \,/\, \mathbf{y}^H B_0\mathbf{x}. \tag{5.21}$$

This result is valid for any sufficiently small matrix perturbations. For the present application, we can exploit the special form of Eqs. (5.14) and (5.15) to further simplify it. As a first step,

since the matrices δA and δB are both proportional to the delay τ, so the eigenvalue perturbation will be also. This clearly makes sense. Furthermore, we can write the eigenvectors $\mathbf{x}$ and $\mathbf{y}$ of the nominal system in block form as

$$\mathbf{x} = \begin{pmatrix} \mathbf{x}_a \\ \mathbf{x}_b \end{pmatrix} \tag{5.22}$$

and

$$\mathbf{y} = \begin{pmatrix} \mathbf{y}_a \\ \mathbf{y}_b \end{pmatrix}, \tag{5.23}$$

where these sub-vectors satisfy

$$\begin{aligned} &\mathbf{x}_a = \lambda \mathbf{x}_b, \\ &[\lambda^2 \overline{M} + \lambda \overline{C} + \overline{K}]\mathbf{x}_b = \mathbf{0} \end{aligned} \tag{5.24}$$

and

$$\begin{aligned} &-\mathbf{y}_a^H \overline{K} = \lambda \mathbf{y}_b^H, \\ &\mathbf{y}_a^H [\lambda^2 \overline{M} + \lambda \overline{C} + \overline{K}] = \mathbf{0}. \end{aligned} \tag{5.25}$$

Eq. (5.22) then reduces to the quite tractable expression

$$\delta\lambda \approx -\lambda\tau \cdot \mathbf{y}_a^H (\tilde{C} + \lambda \tilde{M})\mathbf{x}_b \,/\, [\mathbf{y}_b^H \mathbf{x}_b + \lambda \mathbf{y}_a^H \overline{M} \mathbf{x}_b], \tag{5.26}$$

or equivalently, after multiplying throughout by λ and using (5.19[a]),

$$\delta\lambda \approx -\lambda^2\tau \cdot \mathbf{y}_a^H (\tilde{C} + \lambda \tilde{M})\mathbf{x}_b \,/\, \mathbf{y}_a^H (\lambda^2 \overline{M} - \overline{K})\mathbf{x}_b. \tag{5.27}$$

This can be computed easily for any given structure, so giving both the direction and magnitude of the change to be expected in each closed-loop pole as a result of a specified delay. Examination of that pole which goes unstable most quickly therefore allows an estimate to be made of the critical delay τ^* at which the system will first be expected to become unstable.

Note that Eqs. (5.26) and (5.27) are invariant under scaling of the left and right generalized eigenvectors. It is therefore not necessary to carry out any normalization procedure on these

vectors before computing the eigenvalue perturbation using this expression. The only computational steps required are therefore:

(a) Construct the matrices $\overline{M}$, $\tilde{M}$ and $\tilde{C}$ using (2.9), (3.5) and (3.6), respectively.

(b) Solve for the eigenvectors, using (5.24) and (5.25), for the particular λ of interest.

(c) Compute the scalar expression (5.26) or (5.27).

In most practical applications, the physical structure to be controlled will be very lightly damped. Furthermore, the AVA damping will also generally be chosen to be quite low, as will be further illustrated by the examples in the next section. It is therefore of interest to consider how delays affect the closed-loop eigenvalues in this case. Many of the terms in (5.27) then simplify considerably: in particular, we have that $\lambda \approx j\omega$, $\mathbf{y}_a \approx \mathbf{x}_b$ is approximately real, and $\tilde{M} << \tilde{C}$. We can therefore rewrite (5.27) as

$$\delta\lambda \approx -\omega^2 \tau \cdot \mathbf{x}_b^T \tilde{C} \mathbf{x}_b \,/\, \mathbf{x}_b^T (\omega^2 \overline{M} + \overline{K}) \mathbf{x}_b. \tag{5.28}$$

All terms in this approximation are real, so the eigenvalue perturbation for lightly-damped structures is too. Thus, feedback delays mainly affect only the real parts of the eigenvalues of such systems.

It is interesting to note that feedback delays will not destabilize <u>all</u> modes of the composite system. Instead, what typically occurs is that the low-frequency modes are stabilized, i.e. shifted farther into the left half-plane, while it is only the high-frequency modes that are destabilized. The crossover between these two regimes is just, for the case of a single degree-of-freedom AVA, the natural frequency of the AVA virtual system. (The generalization to multi-degree-of-freedom AVAs is quite straightforward.) This can be shown by means of (5.28) as follows: the matrix $\overline{M}$ is positive definite, so $\omega^2 \overline{M} + \overline{K}$ certainly is also. Thus, the denominator of this equation is guaranteed to be positive. The sign of $\delta\lambda$ will therefore just be the opposite of the

sign of the term $\mathbf{x}_b^T \tilde{C} \mathbf{x}_b$. But, from (2.6) and (5.6), this can be written in terms of the displacements of the physical and virtual structures as

$$\mathbf{x}_b^T \tilde{C} \mathbf{x}_b = -\mathbf{q}^T B \Phi_v diag(\omega_{vi}^2) \boldsymbol{\eta}_v . \tag{5.29}$$

Now, the input to the AVA is just, by (2.3), $\mathbf{u}_v = B^T \ddot{\mathbf{q}}$. Regarding this as a lightly-damped single degree-of-freedom harmonic oscillator, its output η_v will be approximately in phase with its input at frequencies below ω_v, and 180° out-of-phase with it at frequencies above it. But $\mathbf{u}_v$ is itself 180° out-of-phase with the term $B^T \mathbf{q}$, as a result of the double derivative. Thus, (5.29) will be positive at low frequencies and negative at high. This demonstrates that delays do indeed stabilize low-frequency modes while destabilizing the higher-frequency ones.

It should be noted that the results presented here are based on an assumption of distinct closed-loop eigenvalues. If the composite system has repeated frequencies, the first-order eigenvalue perturbation expression (5.18) no longer applies as it stands. Fortunately though, similar results can be still obtained by means of the methods of [20]. The main complication in this case arises from the fact that the eigenvectors corresponding to a set of repeated eigenvalues are not unique; rather, they span a subspace of permissible eigenvectors. There is therefore a degree of non-uniqueness in the definition of the eigenvectors to be used in the first-order eigenvalue perturbation equation. However, it is still possible to define a set of *differentiable eigenvectors* [20] corresponding to the repeated eigenvalues, and these unique vectors can be used to obtain well-defined eigenvector perturbations. Thus, the results obtained here generalize directly to the repeated-eigenvalue case.

A particularly simple, although somewhat conservative, lower bound on the critical delay can be obtained by considering the definiteness of the composite mass and stiffness matrices. As already noted, these matrices are not symmetric once a delay is introduced into the feedback

loop. However, their eigenvalues can be shown to be, to first order, equal to those of their symmetric parts

$$M_s = \tfrac{1}{2}(M_\tau + M_\tau^T) = \overline{M} + \frac{\tau}{2}(\tilde{M} + \tilde{M}^T)$$

and (5.30)

$$C_s = \tfrac{1}{2}(C_\tau + C_\tau^T) = \overline{C} + \frac{\tau}{2}(\tilde{C} + \tilde{C}^T).$$

A sufficient, but not necessary, condition for closed-loop stability is that these matrices both be positive (semi-)definite. Thus, a lower bound on the critical delay is the delay for which either M_s or C_s first has an eigenvalue which crosses the imaginary axis. For lightly-damped systems, it should be noted that the eigenvalues of the nominal damping matrix $\overline{C}$ will be considerably smaller than those of the nominal mass matrix $\overline{M}$. Furthermore, the damping perturbation $\tilde{C}$ is, by (5.5) and (5.6), significantly smaller than the mass perturbation $\tilde{M}$. The damping matrix will therefore become indefinite for a far smaller delay than will the mass matrix; it is consequently the only matrix that need actually be tested.

From (2.9) and (5.6), the symmetric pseudo-damping matrix C_s is given as

$$C_s = \begin{pmatrix} C & 0 \\ 0 & diag(2\zeta_{vi}\omega_{vi}) \end{pmatrix} - \frac{\tau}{2} \cdot \begin{pmatrix} 0 & B\Phi_v diag(\omega_{vi}^2) \\ diag(\omega_{vi}^2)\Phi_v^T B^T & 0 \end{pmatrix}. \tag{5.31}$$

Now, this matrix becomes indefinite when one of its eigenvalues equals zero, i.e. when $\det\{C_s\} = 0$. Making use of the same type of determinantal identity [12] that led to (4.4), this can be rewritten as

$$\det\{C - \tau^2 \cdot B\Phi_v diag(\frac{\omega_{vi}^3}{8\zeta_{vi}})\Phi_v^T B^T\} = 0. \tag{5.32}$$

This matrix can be regarded as the nominal damping matrix C perturbed by a term proportional to the small quantity τ^2. Standard eigenvalue perturbation results [11][21] can therefore be used to predict, to first order, the value of τ for which one of its eigenvalues will equal zero. Suppose

C has eigenvalue μ and corresponding eigenvector $\mathbf{v}$, normalized so as to give $\|\mathbf{v}\|_2 = 1$. (Note that the symmetry of C implies that $\mathbf{v}$ is both the left and right eigenvector corresponding to μ.) Then, a first-order approximation to the perturbation in this eigenvalue is just

$$\delta\mu \approx -\tau^2 \cdot \mathbf{v}^T B\Phi_v diag(\frac{\omega_{vi}^3}{8\zeta_{vi}})\Phi_v^T B^T \mathbf{v}. \tag{5.33}$$

Thus, the delay at which this eigenvalue becomes zero is approximately given as

$$\tau_s \approx \sqrt{\frac{\mu}{\mathbf{v}^T B\Phi_v diag(\frac{\omega_{vi}^3}{8\zeta_{vi}})\Phi_v^T B^T \mathbf{v}}}. \tag{5.34}$$

Considering all eigenvalues of C gives n expressions of this form; the smallest of these is the estimated delay at which indefinite damping is obtained. This expression provides insight into the way in which the AVA gain-like parameter Φ_v affects delay robustness: as $\|\Phi_v\|$ increases, so does the denominator of (5.35). The delay at which C ceases to be positive definite therefore decreases, i.e. the closed-loop system becomes less tolerant to feedback delays. This is certainly physically reasonable.

Equation (5.34) requires only the solution of an (n x n) symmetric eigenproblem, and so is quite attractive computationally. It becomes even simpler if the original physical structure is given in modal form. We then have that $C = diag(2\zeta_i\omega_i)$, so its eigenvalues are just $\{2\zeta_i\omega_i\}$ and its eigenvectors are of the form $(0,\cdots,0,1,0,\cdots,0)^T$. The j^{th} critical delay (5.34) therefore reduces to

$$\tau_{s_j} \approx 4 \cdot \sqrt{\frac{\zeta_j\omega_j}{\mathbf{p}^T diag(\frac{\omega_{vi}^3}{\zeta_{vi}})\mathbf{p}}}, \tag{5.35}$$

where $\mathbf{p} = \Phi_v^T \mathbf{b}_j$ and $\mathbf{b}_j$ is the j^{th} row of B.

6. Examples

The results derived in the previous sections will now be illustrated by application to flexible structures of progressively increasing complexity. The first system considered is a single degree-of-freedom one, i.e. a physical structure consisting of a single mass, spring and dashpot. In this application the disturbance source, primary output sensor and AVA sensor/actuator pair are all necessarily positioned on the single mass, and so are certainly coincident. A modal model of a cantilever beam is then studied, in order to investigate the properties of an AVA when applied to a system with multiple degrees-of-freedom. The AVA sensor/actuator pair is first taken to be coincident with either the single disturbance source or primary output sensor; multiple disturbances are then considered; and then the non-coincident case is investigated. Finally, the effects of feedback delays are studied for both the mass-spring-dashpot and cantilever beam systems.

6.1 Single Degree-of-Freedom System

Consider a single degree-of-freedom physical structure with a natural frequency of $\sqrt{2}$ rad/s and a damping ratio of 0.01. An AVA is required to introduce a transmission zero into this system at the disturbance frequency of 0.6 rad/s; as the system is coincident, this is achieved simply by selecting $\omega_v = 0.6$ rad/s as the natural frequency of the virtual system.

The role of the virtual damping parameter ζ_v can be observed in the closed-loop frequency response plots (Fig. 1) that are obtained for $\zeta_v = 0.001$, 0.1 and 0.2 (and $\Phi_v = 1.5$); the open-loop plot is also given for comparison. A choice of $\zeta_v = 0.1$ thus gives a good compromise between a transmission zero trough that is deep and one that is wide, so providing considerable vibration attenuation over a range of frequencies. The time responses that are obtained for these damping levels (Fig. 2) under harmonic excitation at the disturbance frequency indicate that $\zeta_v = 0.1$ will also give fast transient decay and small steady-state error; this damping ratio is therefore chosen as the design value.

The only parameter remaining to be selected is the scalar Φ_v; this will be chosen in this example so as to minimize the condition numbers of the closed-loop poles, using (3.8) and (3.9). Fig. 3 shows the corresponding plots; a choice of $\Phi_v = 0.8$ yields closed-loop poles which are as robust as possible, and completes the AVA design procedure.

6.2 Coincident Cantilever Beam

As an example of a structure with multiple degrees-of-freedom, consider the transverse vibrational dynamics of a uniform cantilever beam of length 25 m, width 0.1 m and depth 0.01 m, with material properties those of aluminum (density 2.7×10^3 kg/m^3, Young's modulus 7.0×10^{10} N/m^2). The primary displacement sensor is located at the free tip of the beam, and a harmonic disturbance source operating at 0.4 rad/s is positioned 15 m from the built-in end. A 6-mode model of this structure has natural frequencies between 0.0827 and 7.0213 rad/s; this model will be studied here, with a damping ratio of 0.005 assumed for all modes.

An AVA is to be designed to minimize the effects of the disturbance signal on the measured output. A virtual damping ratio of $\zeta_v = 0.10$ will be selected in all the configurations studied, based on the observations of the last sub-section. As a first case, Fig. 4 shows the frequency responses that are obtained by placing the AVA at the disturbance source; the three plots are for values of the gain-like quantity Φ_v of 0 (open-loop), 5 and 10. It can be seen that increasing the gain increases both the depth and width of the virtual zero trough, as should be expected. Furthermore, the three higher-frequency structural zeros clearly do not shift from their open-loop values; this agrees with the result proved earlier for coincident systems. Fig. 5 then shows the variation of the LQR-like objective function J of (3.7) with Φ_v; a control weighting of $\rho = 0.15$ was used. A choice of $\Phi_v = 3.3$ is thus optimal in this sense, and can be taken as the design value.

Fig. 6 is analogous to Fig. 4, but with the AVA now coincident with the primary output sensor rather than the disturbance source. The basic properties of these two configurations are quite similar, although the details can be seen to differ somewhat. Fig. 7 then shows the closed-loop output obtained in the latter case in response to the harmonic disturbance excitation, which has unit amplitude; a fairly high value of $\Phi_v = 7$ is used in order to ensure good output regulation. The effectiveness of the AVA in absorbing the sinusoidal excitation can clearly be seen.

Finally, the use of a single AVA to absorb two distinct disturbance signals will be illustrated. A second harmonic disturbance acting at 2.0 rad/s is applied to the beam at a location 7.5 m from the built-in end, and a two degree-of-freedom AVA positioned coincident with the primary output sensor. The natural frequencies of the virtual structure in this case are just the two disturbance frequencies, and the virtual modal parameter Φ_v is now a (1 x 2) vector. Fig. 8 shows the closed-loop frequency responses from each of the two disturbance stations to the measured output that result for a choice of $\Phi_v = (7 \quad 5)$. Fig. 9 then gives the corresponding closed-loop time response obtained if the first disturbance has a peak amplitude of 1 and the second 2. By comparison with the open-loop response (which clearly exhibits the effect of the high-frequency input: see Fig. 7), the AVA can be seen to again produce very acceptable rejection in this multi-disturbance case.

6.3 Non-Coincident Cantilever Beam

We shall now briefly illustrate of the design of a single-mode AVA with a sensor/actuator pair which is not coincident with either the disturbance or output. Consider the same cantilever beam as before, with the primary sensor still at the free tip. However, the AVA is now located 10 m from the built-in end, and a disturbance source of unspecified frequency is positioned at 15 m. Equation (4.9) is then used to determine the required AVA natural frequency and damping ratio as the disturbance frequency ranges over all possible values; in all cases, a damping ratio of 0.1 is specified for the virtual zero. Fig. 10 shows the resulting virtual frequency ω_v versus

disturbance frequency for a choice of $\Phi_v = 7$, and Fig. 11 gives the corresponding ζ_v plot. It can be seen that the only large perturbations occur in the vicinity of the structural zero near 1 rad/s, as predicted. Finally, Fig. 12 shows the resulting closed-loop frequency response plot produced by this non-coincident controller, together with the open-loop plot for comparison. The AVA can be seen to have indeed introduced a zero at the desired frequency.

6.4 Effects of Delays

The remaining six plots illustrate the closed-loop stability properties of the two structures discussed above when a small delay is present in the AVA feedback loop. The mass-spring-dashpot system AVA is chosen in this case to have virtual modal parameters $\omega_v = 1.0$ rad/s, $\zeta_v = 0.02$, and either $\Phi_v = 1$ (referred to as the *low gain* case) or $\Phi_v = 3$ (*high gain*). The resulting loci of closed-loop poles as a function of the delay τ are given in Figures 13 and 14. In both plots, the poles obtained for $\tau = 0$ are indicated by 'o's. It can be seen that the lower-frequency AVA mode is stabilized in both cases by the introduction of the feedback delay, while the higher-frequency mode is destabilized. This behavior is indeed of the type predicted by (5.29). Furthermore, the low gain system becomes unstable for a delay of 0.076 s and the high gain one for 0.048 s. This agrees with the expectation that the critical delay will decrease with increasing AVA control gain. Figure 15 provides further information on this point by plotting against control gain Φ_v the actual critical delay (solid curve); that predicted by the eigenvalue perturbation expression (5.27) (dashed plot); and the simple conservative bound obtained from the damping matrix (5.35) (dotted plot). The very close agreement between the true critical delay and that predicted by (5.27) can be easily seen, as can the general trend of decreasing delay with increasing Φ_v. It can also be seen that the values of critical delay are considerably smaller than the periods of the two modes of this system; this confirms that the first-order assumption made in (5.1) is indeed acceptable.

Finally, Figures 16 - 18 are analogous to Figures 13 - 15, but for the 6-mode cantilever beam model discussed above. The AVA in this case is positioned at the free end of the beam, with modal parameters taken to be exactly as for the mass-spring-dashpot delay studies. It can be seen from Figures 16 and 17 that the low-frequency modes are again stabilized by delays and the high-frequency ones destabilized, as predicted. In addition, it is important to note that the highest mode is not actually the critical one for this system. It is therefore necessary to test (5.27) for each of the modes with frequencies above the AVA frequency. (If a multi-degree-of-freedom AVA were employed, modes with frequencies lying between the AVA frequencies would also have to be checked.) Lastly, Figure 18 demonstrates the same close agreement between true critical delay and that predicted from the eigenvalue perturbation results as was obtained for the mass-spring-dashpot system. The only significant difference is the slight discontinuity in the beam critical delay curve for a gain of approximately 4.3. The explanation of this is simply that a different mode becomes the critical one for gains higher than this value. This again reflects the fact that all higher-frequency modes are potentially destabilized by delays, and so should be tested by means of the perturbation expression (5.27).

7. Conclusions

This paper has analyzed the properties of virtual passive controllers (active vibration absorbers), and of the closed-loop systems achievable by means of such compensation. In particular, it was shown that these controllers introduce additional transmission zeros into the closed-loop system; they therefore provide an extra degree of design freedom over that provided by state feedback, which cannot alter the zeros in any way.

The control design problem of providing good vibration at a specified frequency, for instance that of a disturbance, is equivalent to requiring that a zero be added at this frequency. Techniques were developed for designing a virtual passive controller to achieve this goal; these methods were shown to be particularly straightforward in the case where the controller sensor/actuator pairs are coincident with either the disturbance sources or the primary output sensors. Methods were then derived for exploiting the remaining controller design freedom to achieve desired secondary objectives, for instance making the closed-loop poles as robust as possible.

Finally, the effects on closed-loop stability of small delays in the feedback loop were investigated. It was shown that these delays tend to destabilize the higher-frequency modes while actually making the lower-frequency ones more heavily damped. Eigenvalue perturbation results were then derived which allow accurate predictions to be made of the critical delay at which instability first occurs. These points were illustrated by simple examples.

References

[1] S.M. Joshi, *Control of Large Flexible Space Structures*, Springer-Verlag, Heidelberg, 1989.

[2] J.N. Juang and M. Phan, 'Robust Controller Designs for Second-Order Dynamic Systems: A Virtual Passive Approach', NASA Technical Memorandum 102666, NASA Langley Research Center, May 1990, and to appear, *Journal of Guidance, Control, and Dynamics*.

[3] K.A. Morris and J.N. Juang, 'Dissipative Controller Designs for Second-Order Dynamic Systems', NASA Contractor Report 187452/ ICASE Report 90-65, NASA Langley Research Center, Sept. 1990.

[4] T.W.C. Williams, 'Transmission Zero Bounds for Large Space Structures, with Applications', *Journal of Guidance, Control, and Dynamics*, **12**, 33-48 (1989).

[5] T. Kailath, *Linear Systems*, Prentice-Hall, Englewood Cliffs, 1980.

[6] T.W.C. Williams and J.N. Juang, 'Pole/Zero Cancellations in Flexible Space Structures', *Journal of Guidance, Control, and Dynamics*, **13**, 684-690 (1990).

[7] G.H. Golub and C.F. Van Loan, *Matrix Computations*, Johns Hopkins University Press, Baltimore, 1983.

[8] W.A. Wolovich, *Linear Multivariable Systems*, Springer-Verlag, New York, 1974.

[9] T.W.C. Williams, 'Computing the Transmission Zeros of Large Space Structures', *IEEE Transactions on Automatic Control*, **34**, 92-94, (1989).

[10] R.V. Patel, 'On Transmission Zeros and Dynamic Output Feedback', *IEEE Transactions on Automatic Control*, **23**, 741-742 (1978).

[11] J.H. Wilkinson, *The Algebraic Eigenvalue Problem*, Oxford University Press, Oxford, 1965.

[12] F.R. Gantmacher, *The Theory of Matrices*, Chelsea Publishing Co., New York, 1959.

[13] T.W.C. Williams, 'Transmission Zeros and High-Authority/Low-Authority Control of Flexible Space Structures', to appear, *Journal of Guidance, Control, and Dynamics*.

[14] T.W.C. Williams, M. Mostarshedi and A. Das, 'Optimum Damper Placement for Flexible Spacecraft: Application to the ASTREX Structure', presented at AIAA Guidance, Navigation and Control Conference, Hilton Head, South Carolina, Aug. 1992.

[15] S. Wolfram, *Mathematica: A System for Doing Mathematics by Computer*, Addison-Wesley, New York, 1988.

[16] A.M. Bruner, W.K. Belvin, L.G. Horta, and J.N. Juang, 'Active Vibration Absorber for the CSI Evolutionary Model: Design and Experimental Results', presented at 32nd AIAA/AHS Structures, Structural Dynamics and Materials Conference, Baltimore, Maryland, Apr. 1991, and to appear, *Journal of Guidance, Control, and Dynamics*.

[17] W.K. Belvin, 'Second-Order State Estimation Experiments using Acceleration Measurements', presented at 33rd AIAA/AHS Structures, Structural Dynamics and Materials Conference, Dallas, Texas, Apr. 1992.

[18] G.W. Stewart and J. Sun, *Matrix Perturbation Theory*, Academic Press, London, 1990.

[19] T.W.C. Williams, J. Xu and J.N. Juang, 'Design Of Virtual Passive Controllers for Flexible Space Structures', presented at AIAA/AAS Astrodynamics Conference, Hilton Head, South Carolina, Aug. 1992.

[20] J.N. Juang, P. Ghaemmaghami and K.B. Lim, 'Eigenvalue and Eigenvector Derivatives of a Non-Defective Matrix', *Journal of Guidance, Control, and Dynamics*, **12**, 480-486 (1989).

[21] G.W. Stewart, *Introduction to Matrix Computations*, Academic Press, New York, 1973.

[22] J. Xu, *Disturbance Isolation and Robust Active Vibration Control*, Ph.D. Dissertation, Department of Aerospace Engineering, University of Cincinnati, 1993.

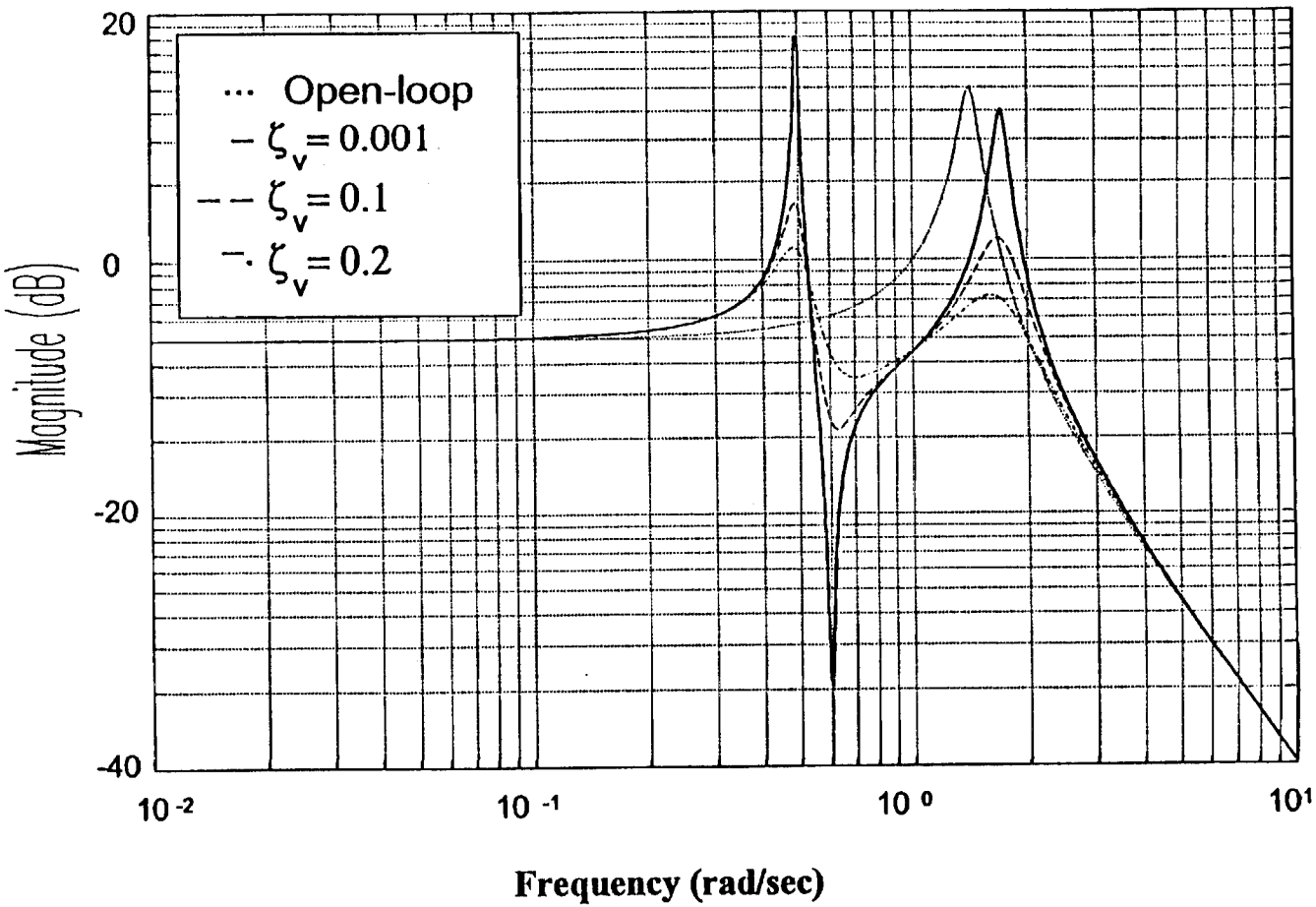

Figure 1 1-DOF system frequency responses.

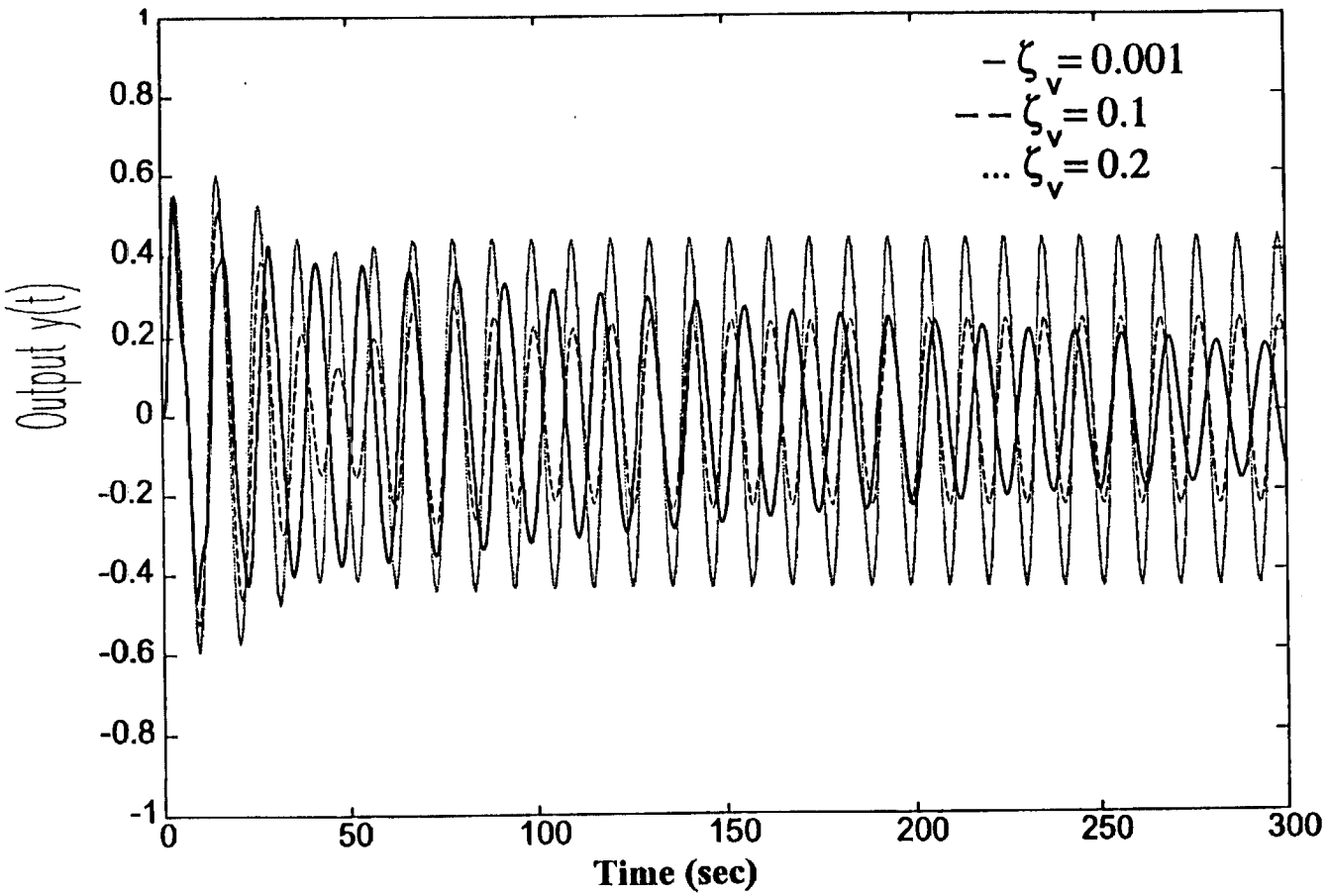

Figure 2 1-DOF system time responses.

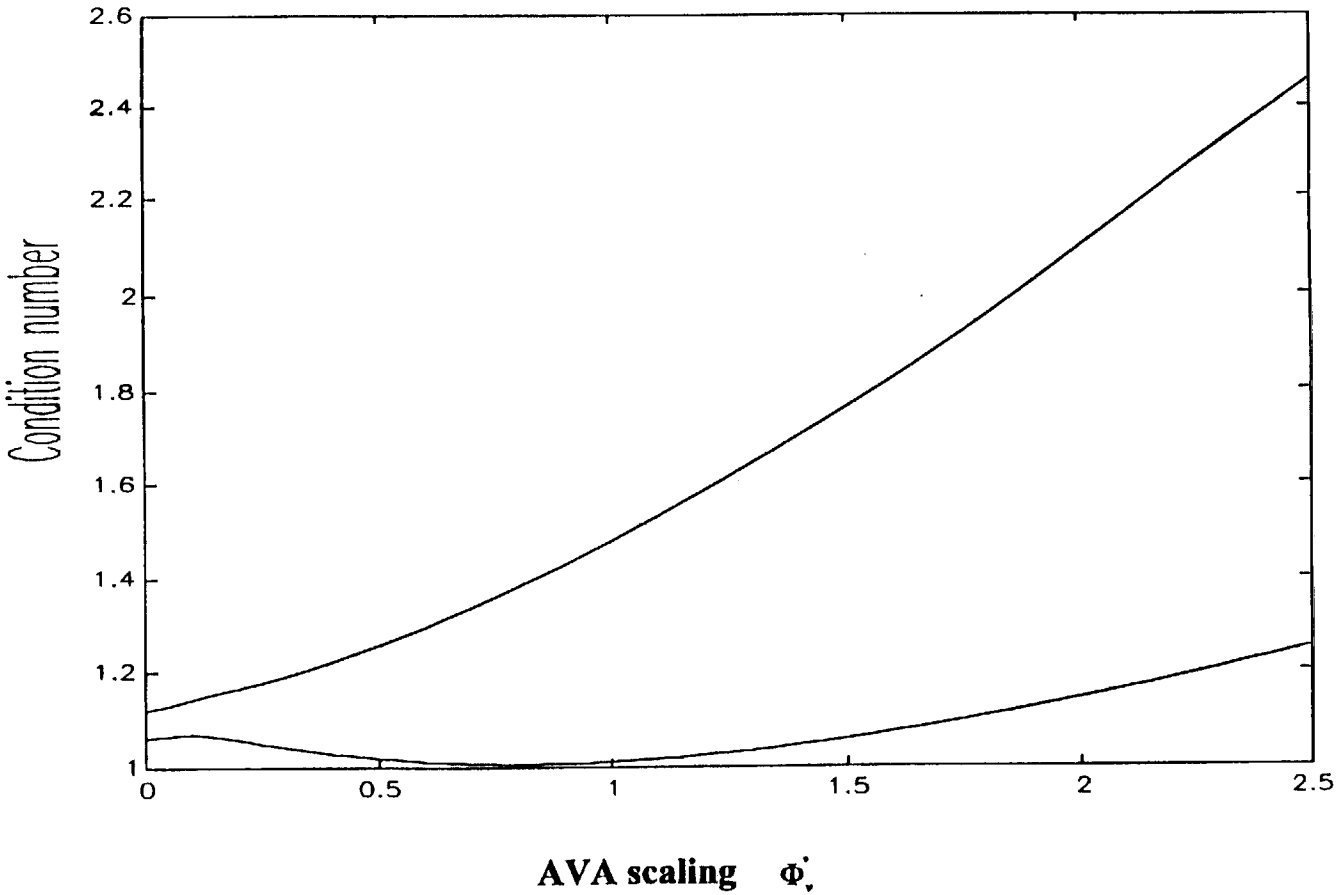

Figure 3 Closed-loop pole condition numbers.

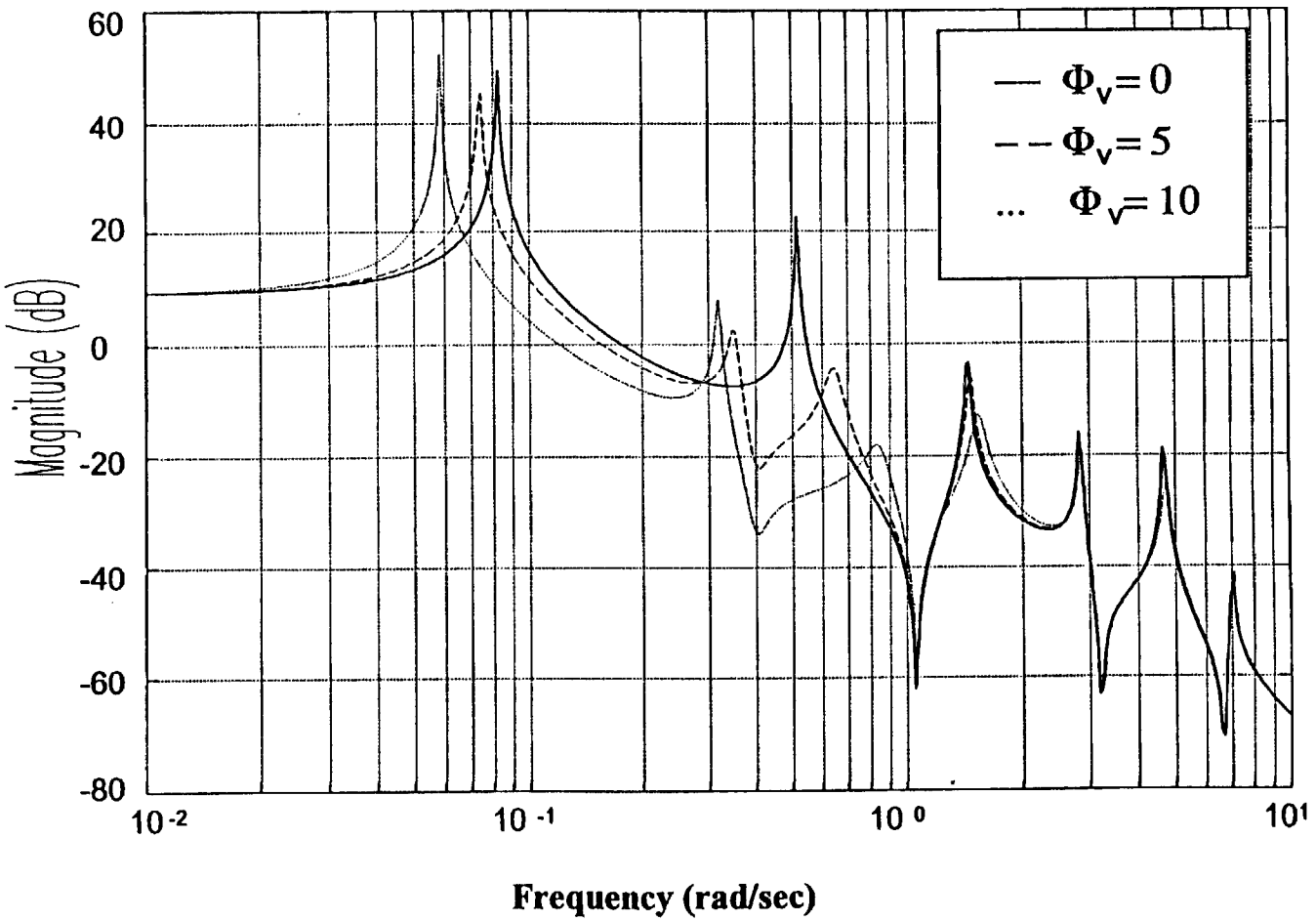

Figure 4 Frequency responses, AVA at disturbance.

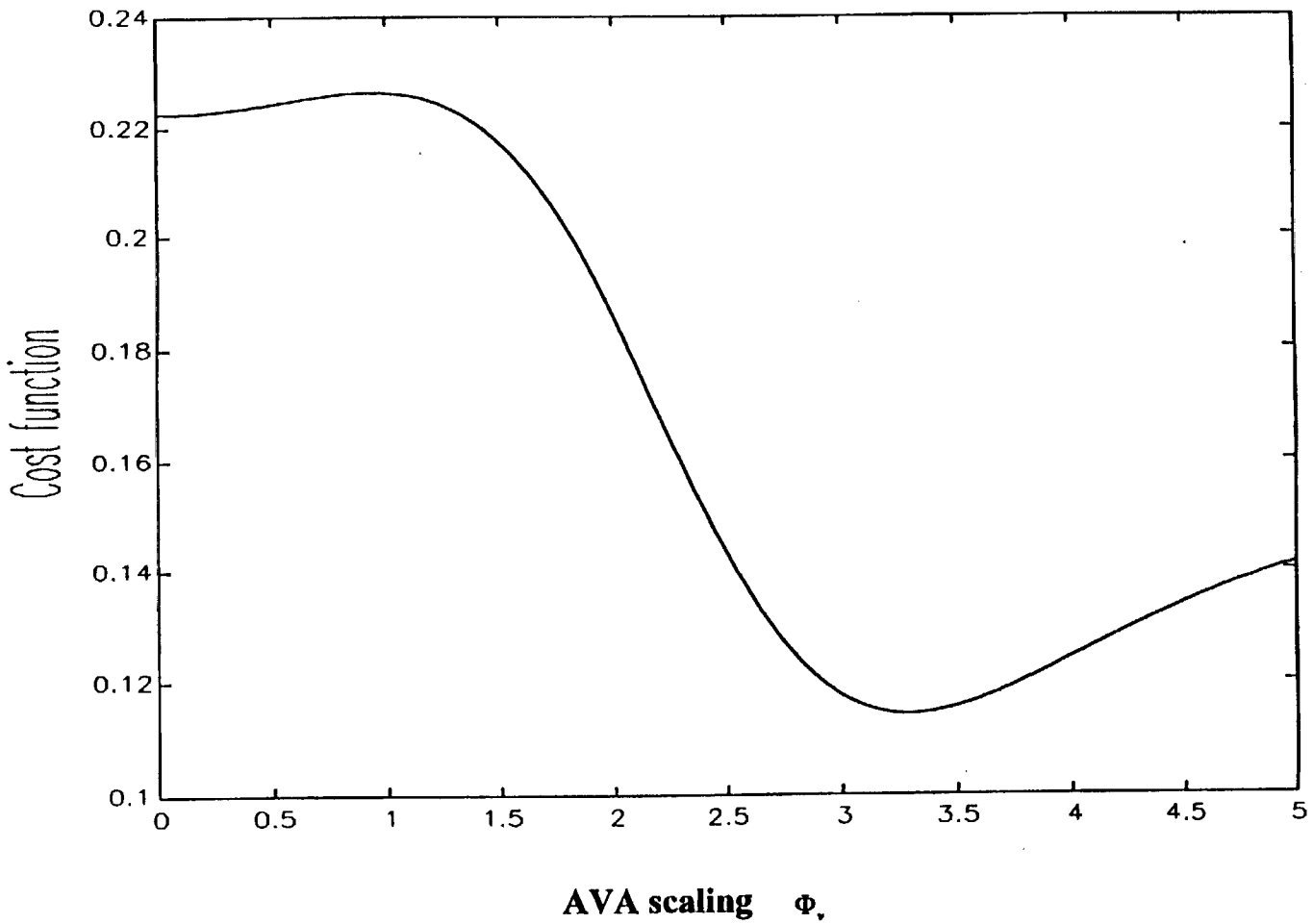

Figure 5 LQR-like objective function.

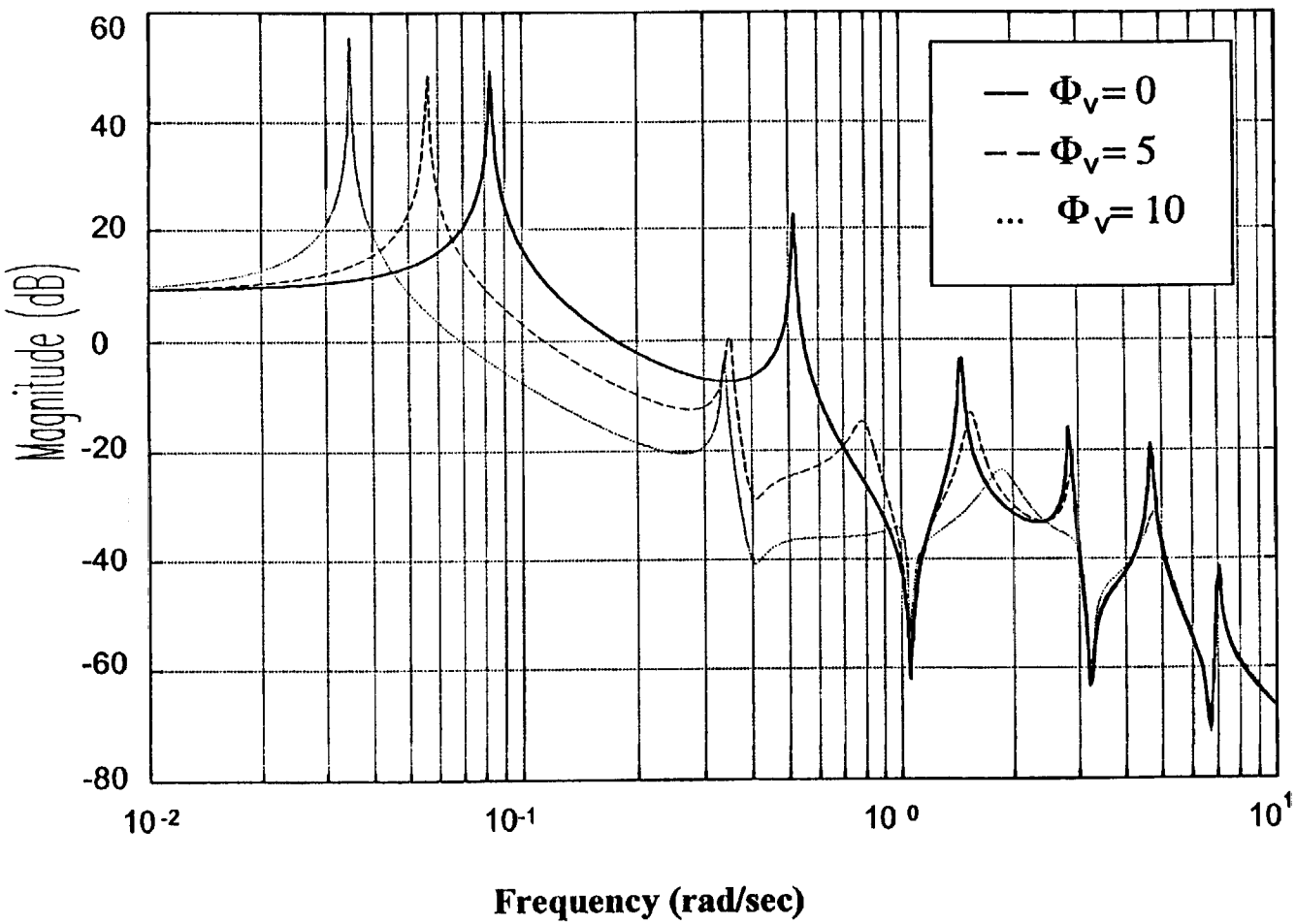

Figure 6 Frequency responses, AVA at beam tip.

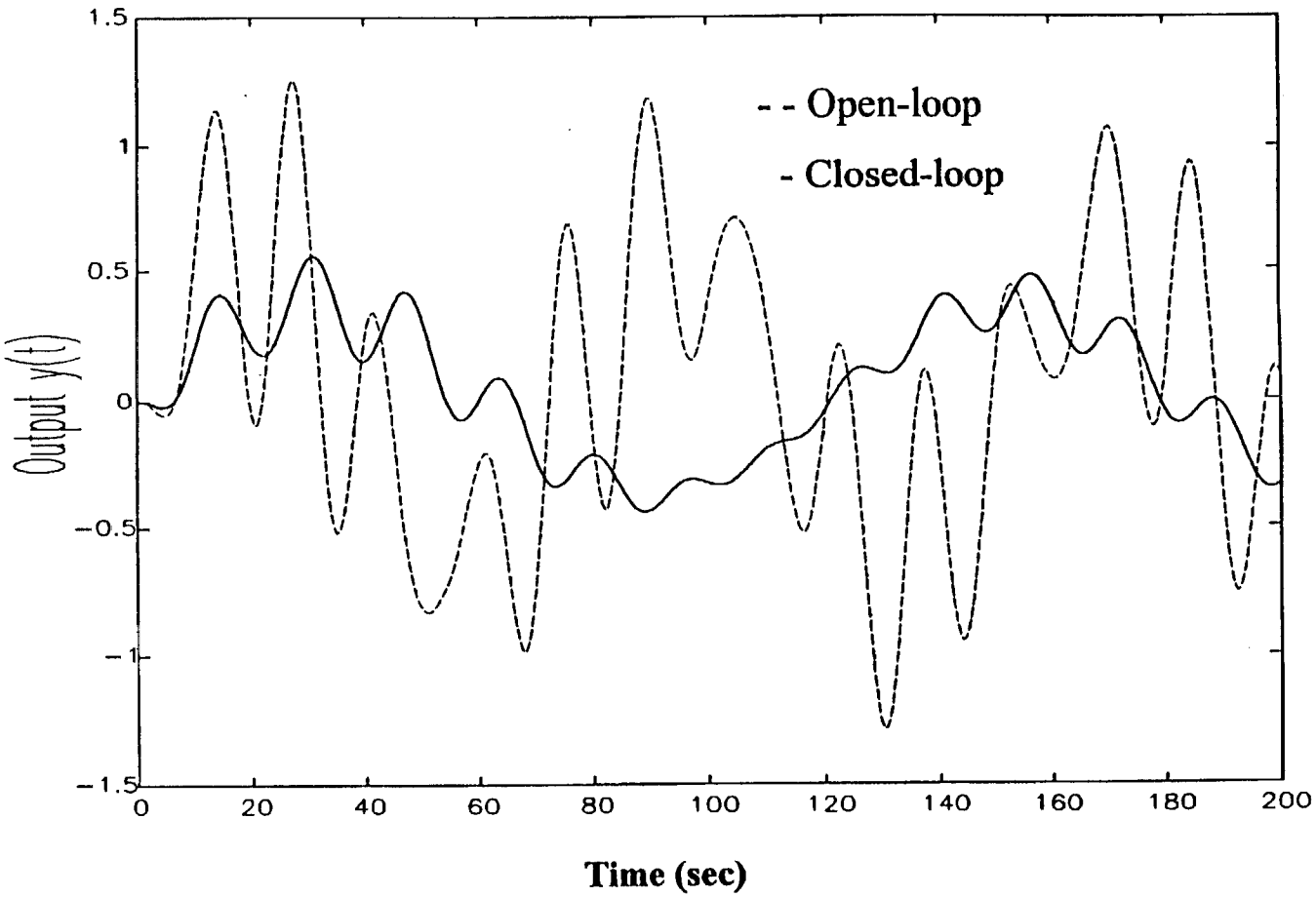

Figure 7 Time responses, AVA at beam tip.

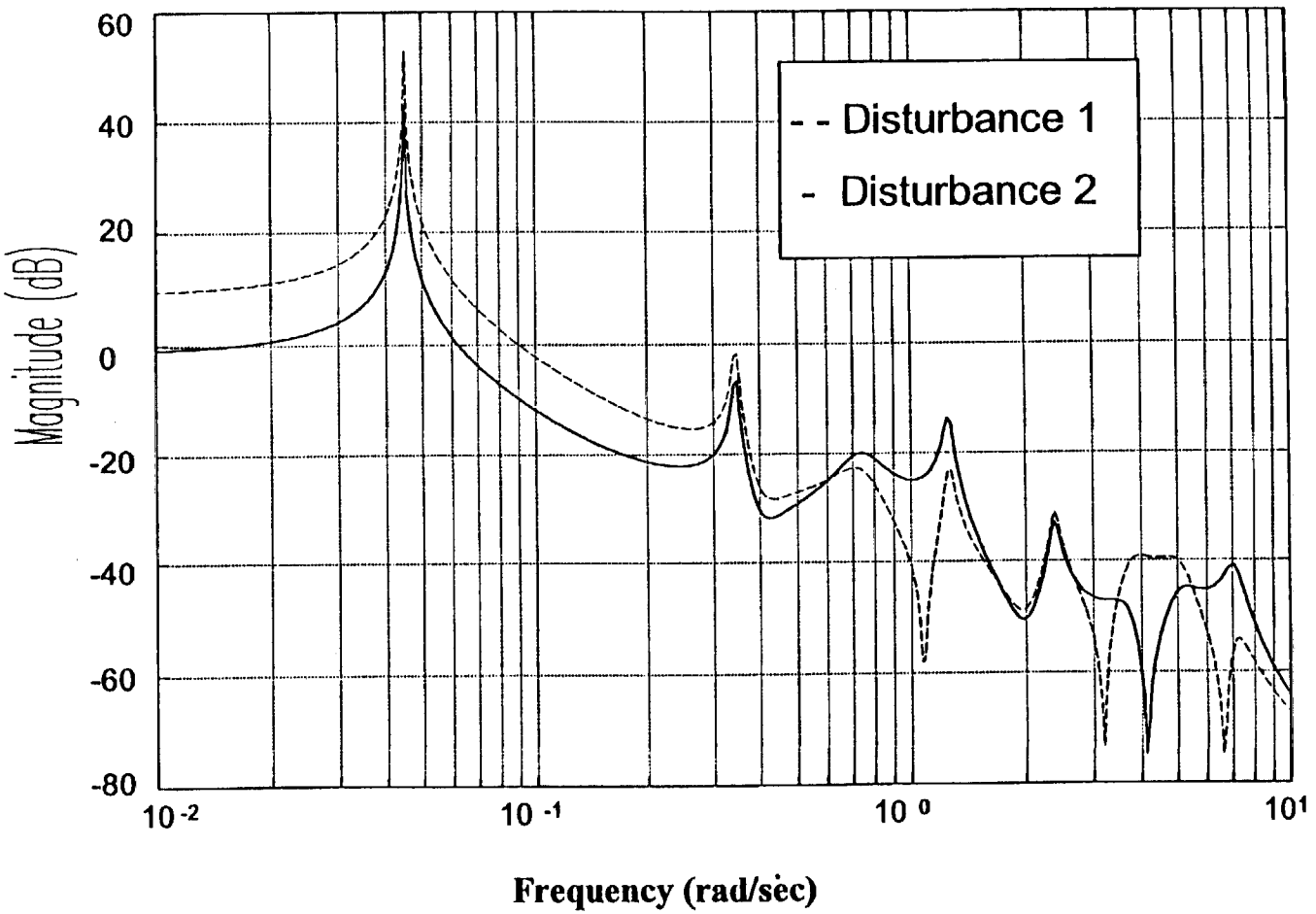

Figure 8 Frequency responses, two disturbances.

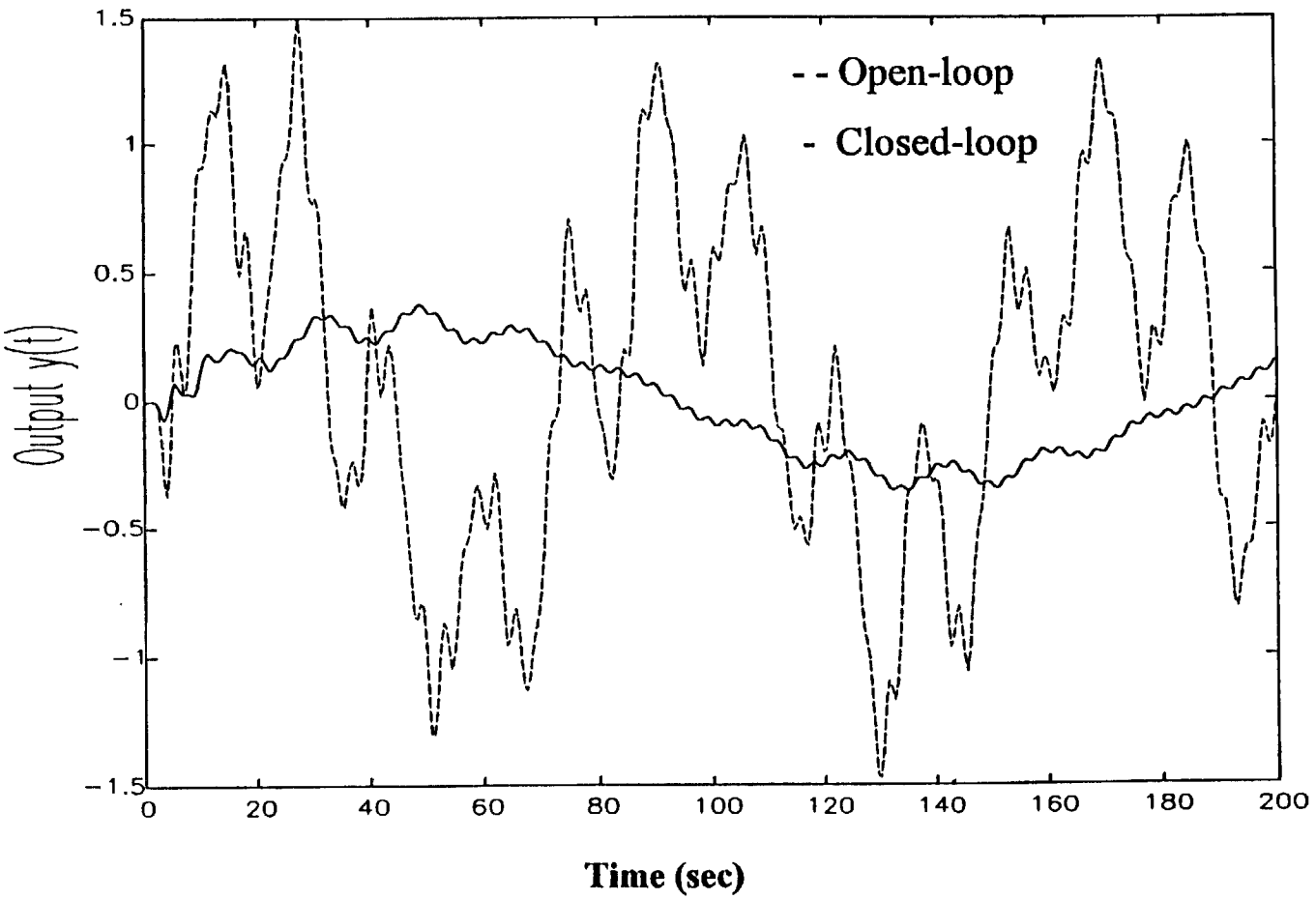

Figure 9 Time responses, two disturbances.

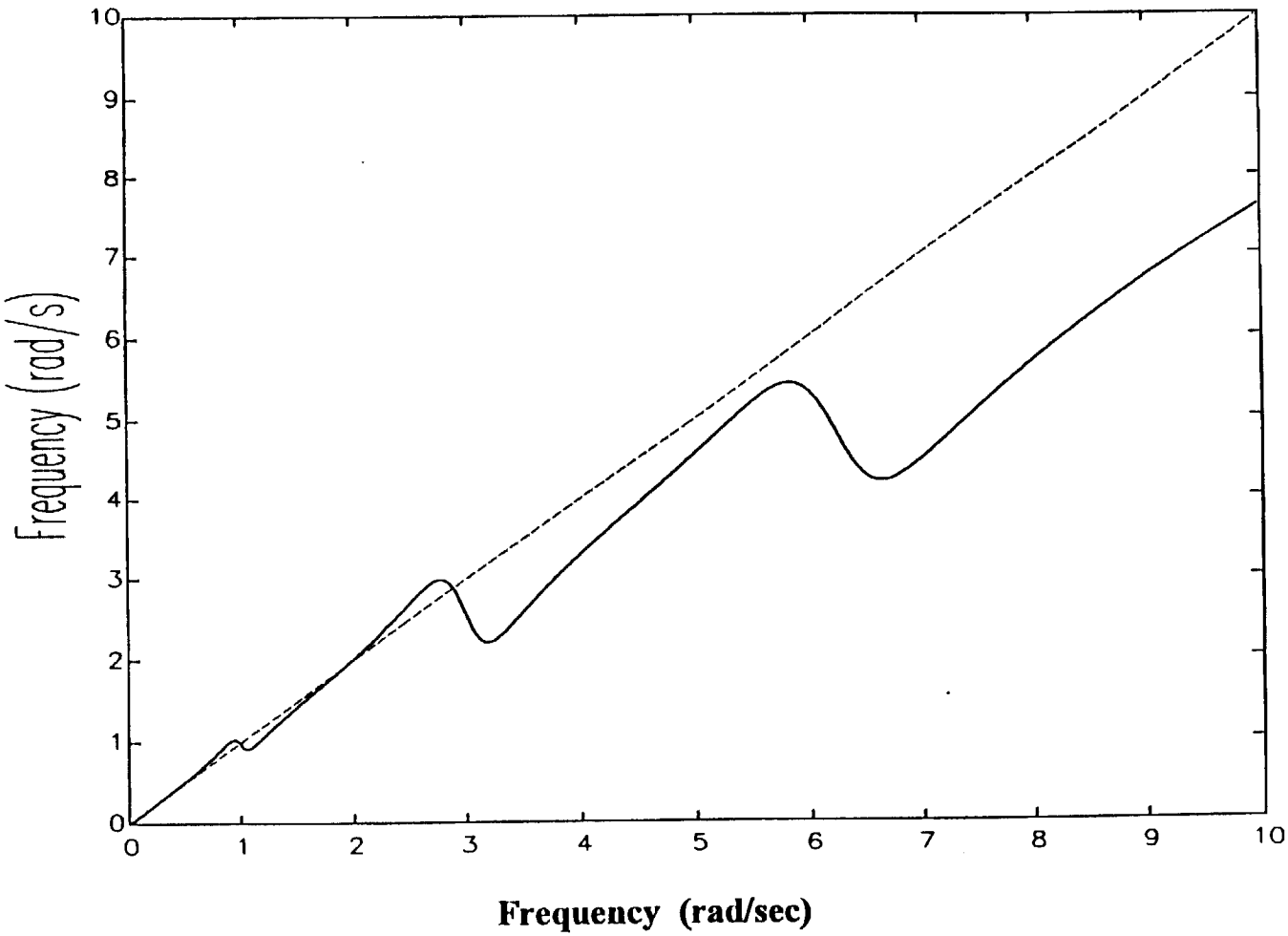

Figure 10 Virtual frequency, non-coincident.

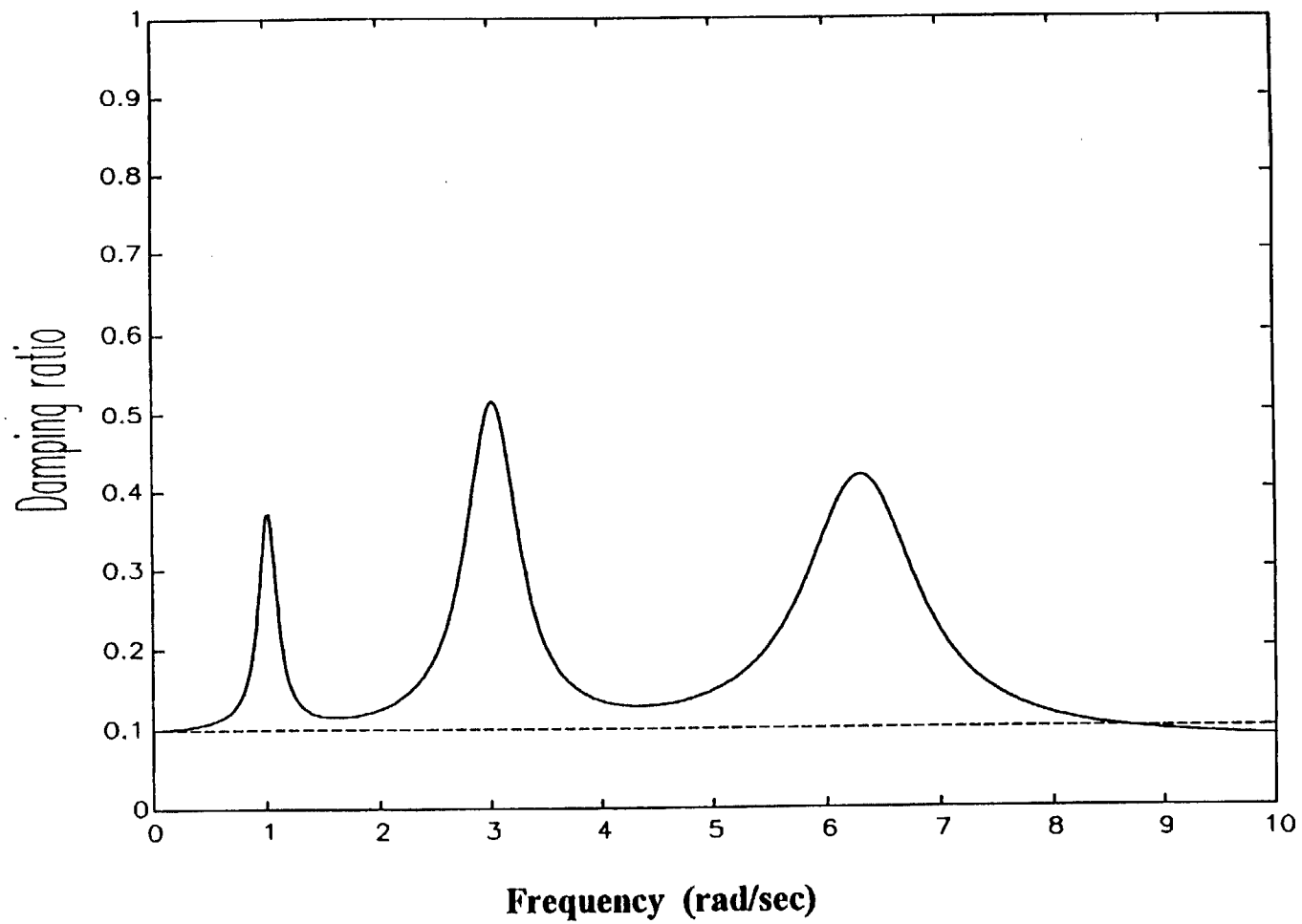

Figure 11 Virtual damping ratio, non-coincident.

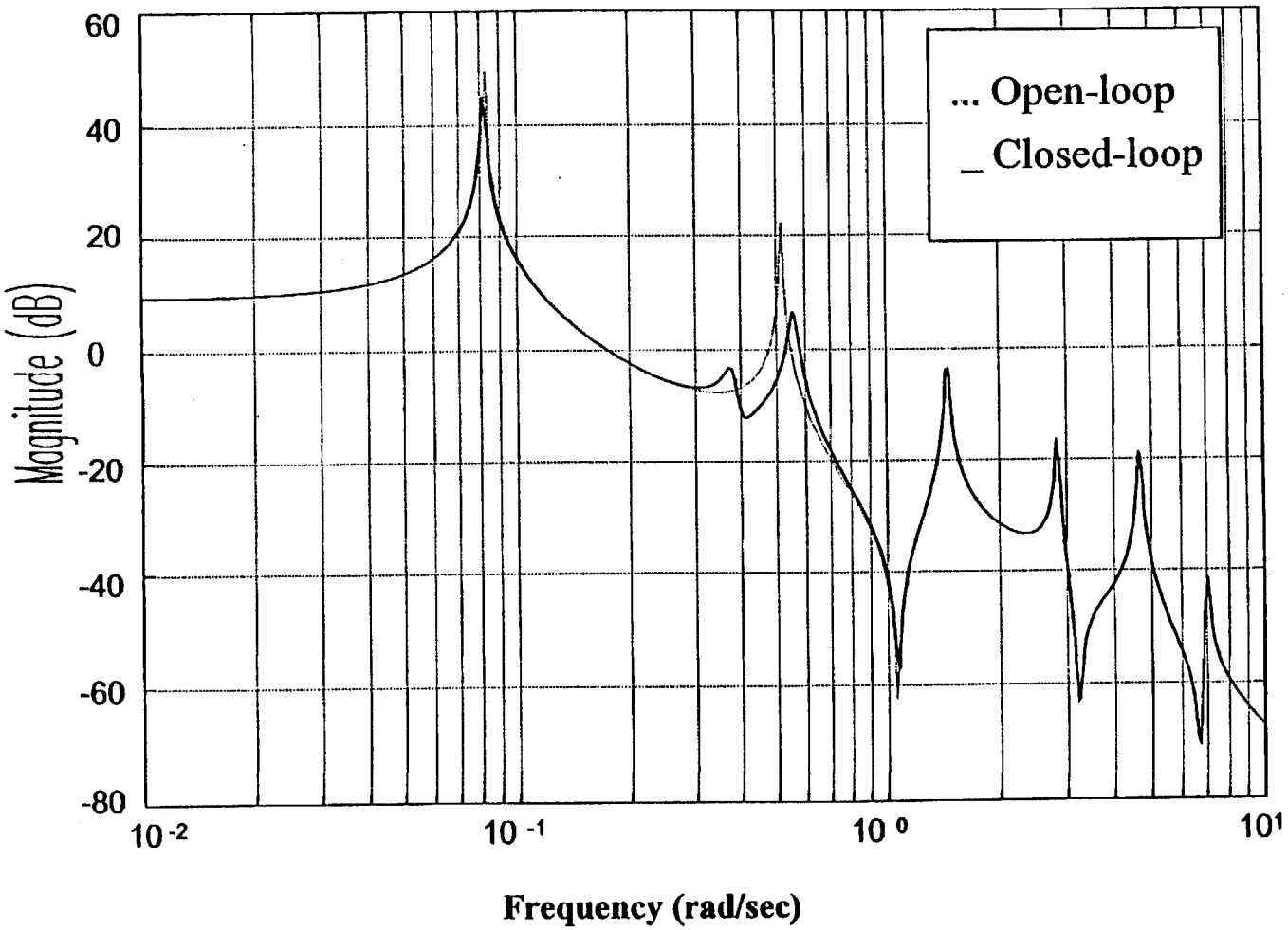

Figure 12 Frequency responses, non-coincident.

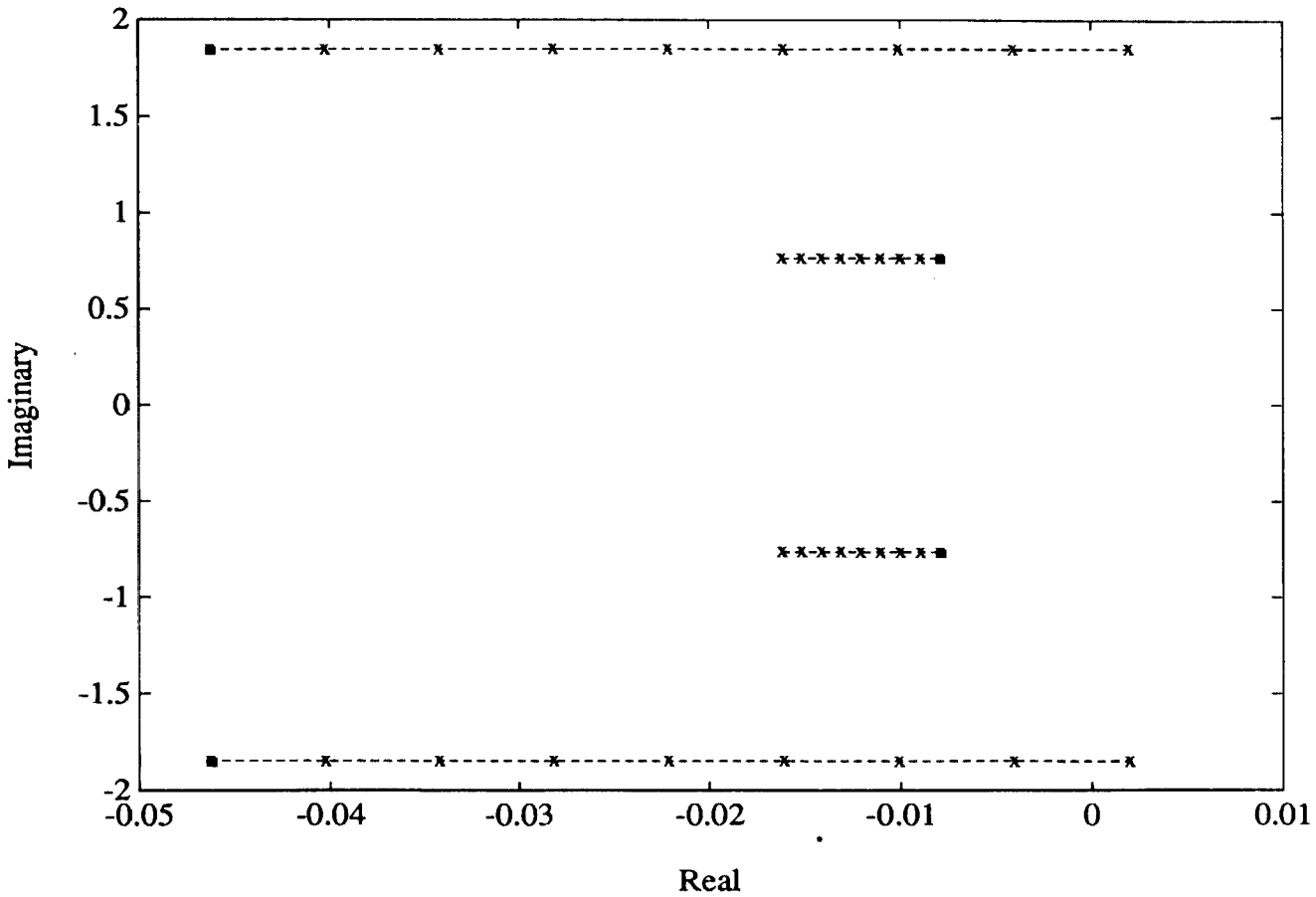

Figure 13 1-DOF root locus against delay, low gain.

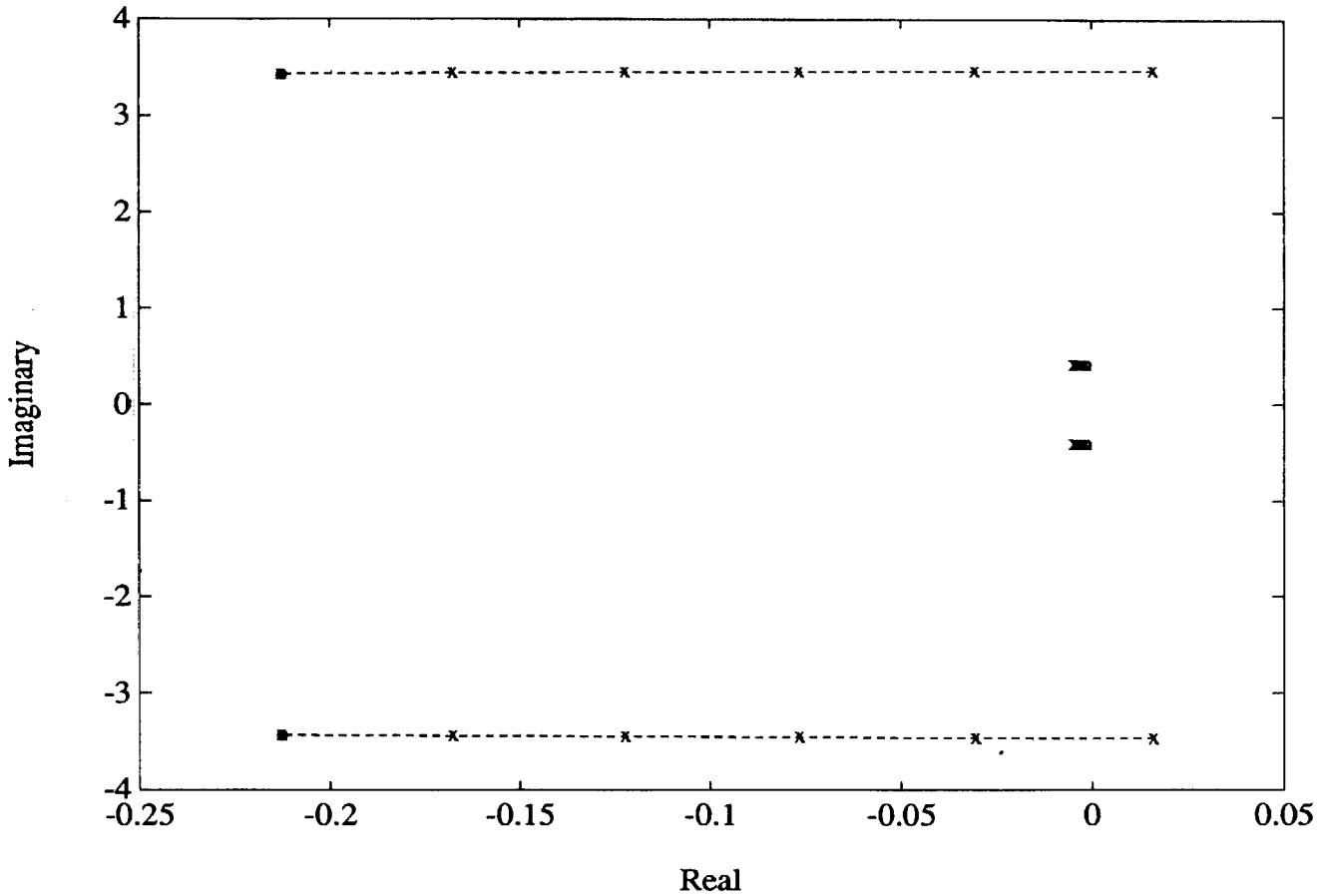

Figure 14 1-DOF root locus against delay, high gain.

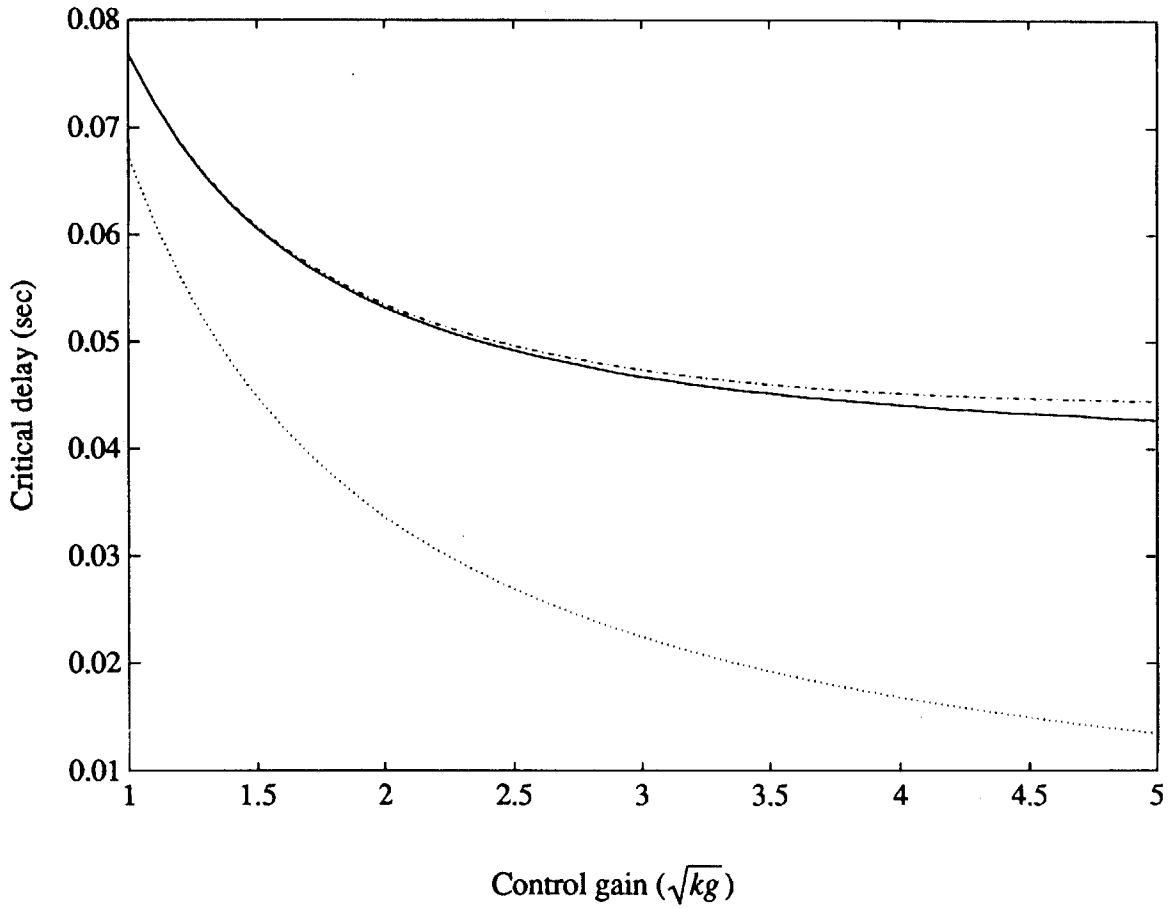

Figure 15 1-DOF critical delay estimates.

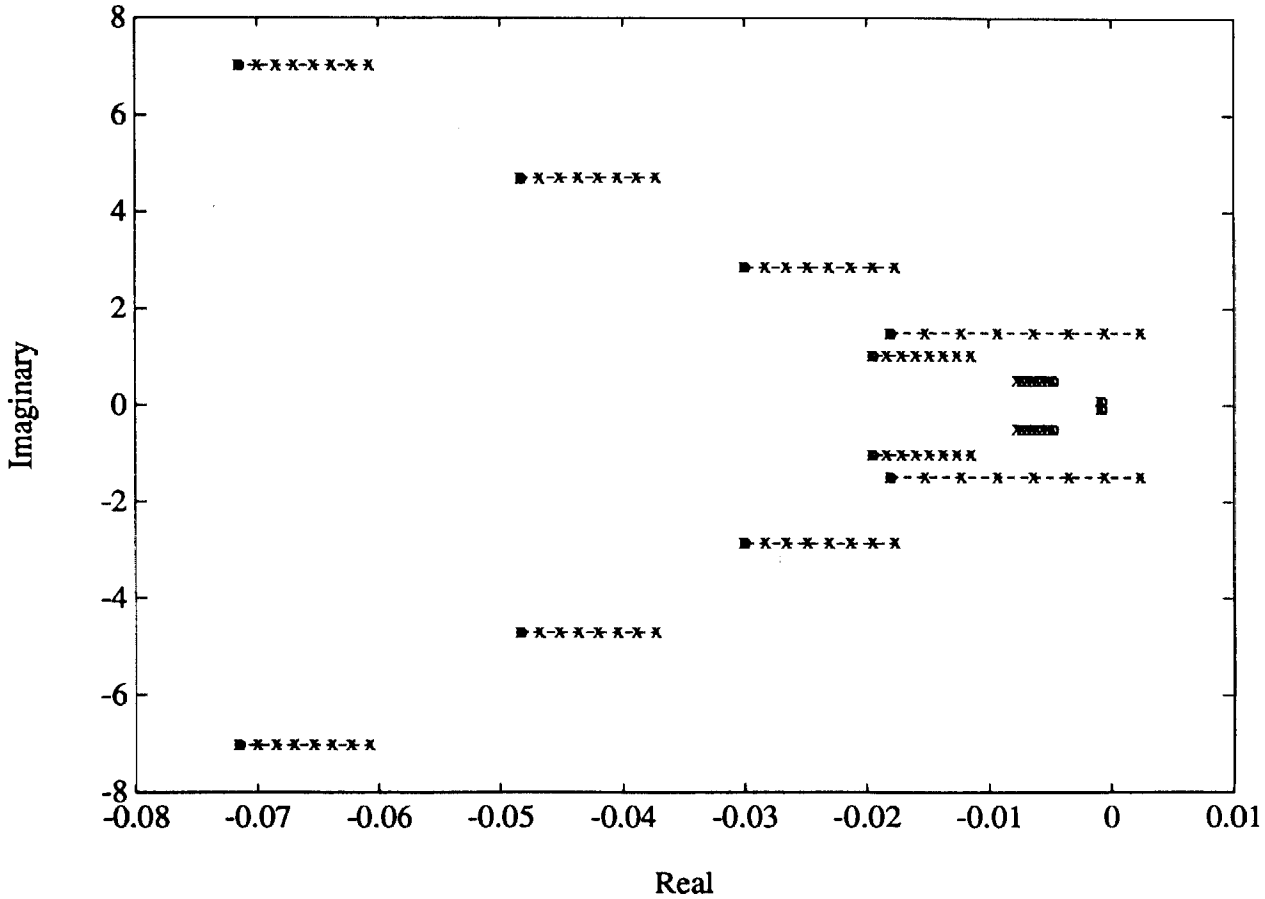

Figure 16 Beam root locus against delay, low gain.

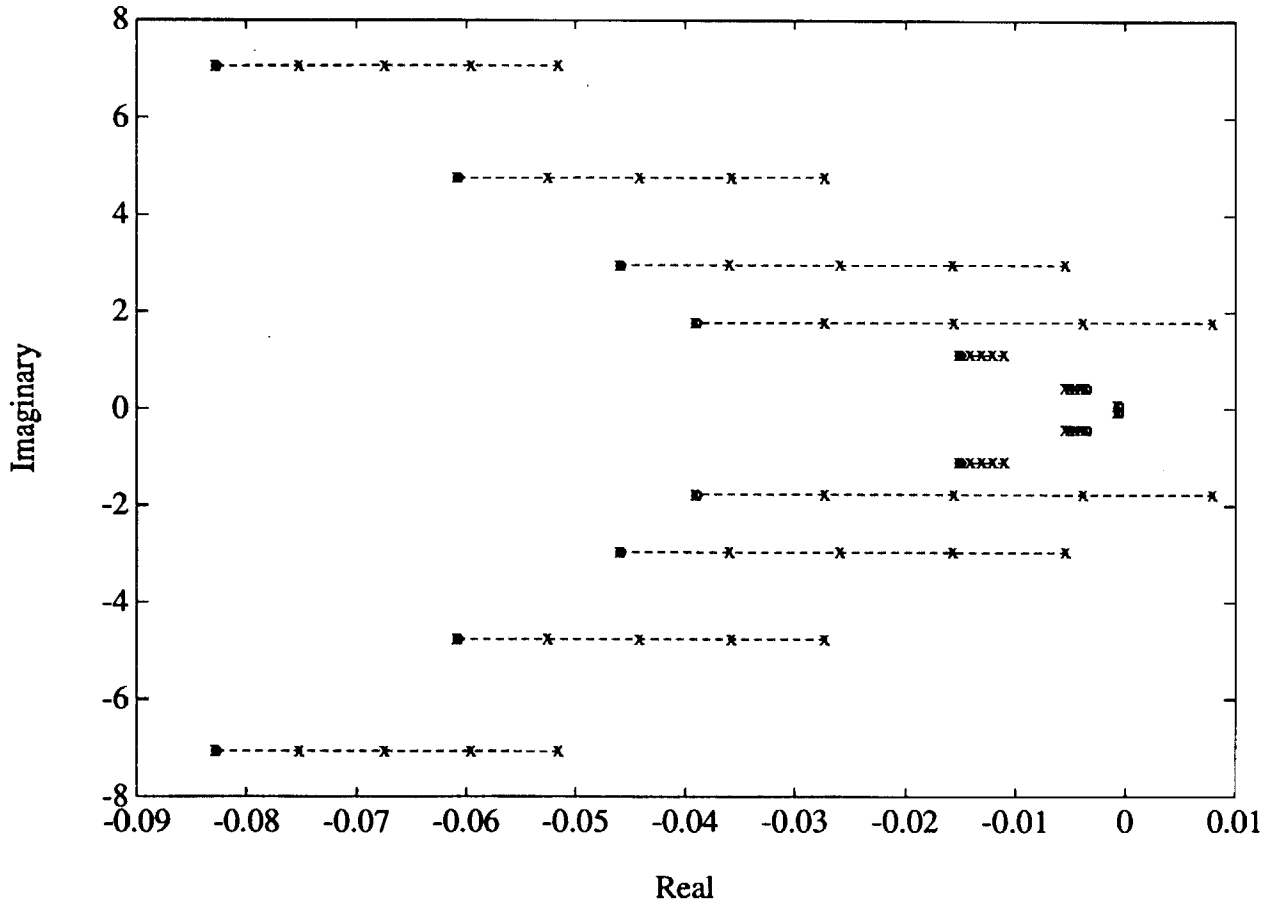

Figure 17 Beam root locus against delay, high gain.

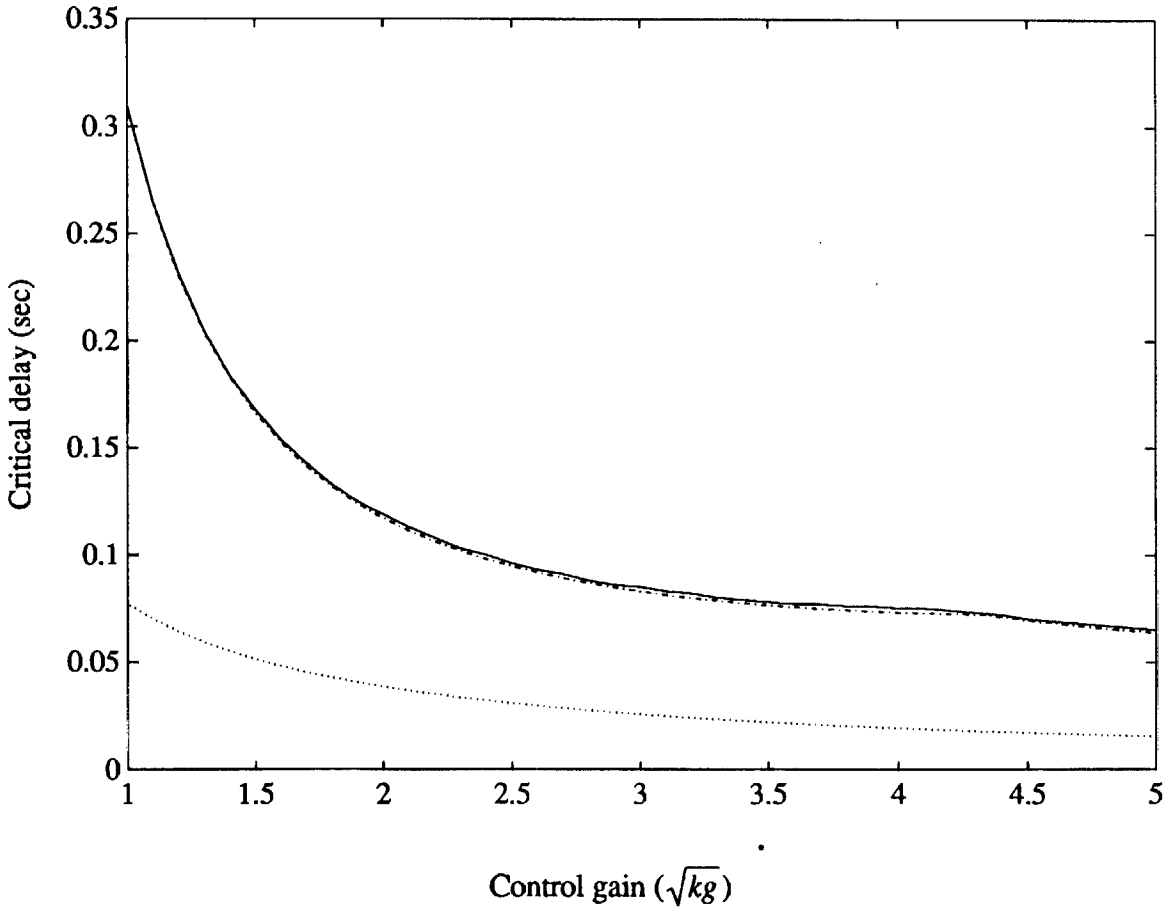

Figure 18 Beam critical delay estimates.